การประเมินสมรรถนะการควบคุมของระบบกังหันลมโดยวิธีเชิงข้อมูลทางสถิติ

นายจตุรวิทย์ ชินจิตร์

จุฬาลงกรณ์มหาวิทยาลัย
Chulalongkorn University

บทคัดย่อและแฟ้มข้อมูลฉบับเต็มของวิทยานิพนธ์ตั้งแต่ปีการศึกษา 2554 ที่ให้บริการในคลังปัญญาจุฬาฯ (CUIR)
เป็นแฟ้มข้อมูลของนิสิตเจ้าของวิทยานิพนธ์ ที่ส่งผ่านทางบัณฑิตวิทยาลัย
The abstract and full text of theses from the academic year 2011 in Chulalongkorn University Intellectual Repository (CUIR)
are the thesis authors' files submitted through the University Graduate School.

วิทยานิพนธ์นี้เป็นส่วนหนึ่งของการศึกษาตามหลักสูตรปริญญาวิศวกรรมศาสตรมหาบัณฑิต
สาขาวิชาวิศวกรรมเคมี ภาควิชาวิศวกรรมเคมี
คณะวิศวกรรมศาสตร์ จุฬาลงกรณ์มหาวิทยาลัย
ปีการศึกษา 2558
ลิขสิทธิ์ของจุฬาลงกรณ์มหาวิทยาลัย

CONTROL PERFORMANCE ASSESSMENT OF WIND TURBINE BY STOCHASTIC METHOD

Mr. Chaturawit Chinnachit

A Thesis Submitted in Partial Fulfillment of the Requirements
for the Degree of Master of Engineering Program in Chemical Engineering
Department of Chemical Engineering
Faculty of Engineering
Chulalongkorn University
Academic Year 2015
Copyright of Chulalongkorn University

Thesis Title	CONTROL PERFORMANCE ASSESSMENT OF WIND TURBINE BY STOCHASTIC METHOD
By	Mr. Chaturawit Chinnachit
Field of Study	Chemical Engineering
Thesis Advisor	Associate Professor Dr.Soorathep Kheawhom, Ph.D.

Accepted by the Faculty of Engineering, Chulalongkorn University in Partial Fulfillment of the Requirements for the Master's Degree

.....Dean of the Faculty of Engineering
(Associate Professor Dr.Supot Teachavorasinskun, Ph.D.)

THESIS COMMITTEE

.....Chairman
(Professor Dr.Paisan Kittisupakorn, Ph.D.)
.....Thesis Advisor
(Associate Professor Dr.Soorathep Kheawhom, Ph.D.)
.....Examiner
(Assistant Professor Dr.Amornchai Arpornwichanop, D.Eng.)
.....External Examiner
(Dr.Pornchai Bumroongsri, D.Eng.)

จตุรวิทย์ ชินจิตร์ : การประเมินสมรรถนะการควบคุมของระบบกังหันลมโดยวิธีเชิงข้อมูลทางสถิติ (CONTROL PERFORMANCE ASSESSMENT OF WIND TURBINE BY STOCHASTIC METHOD) อ.ที่ปรึกษาวิทยานิพนธ์หลัก: รศ. ดร. สุรเทพ เขียวหอม, 68 หน้า.

งานวิจัยนี้นำเสนอเทคนิคการประเมินสมรรถนะการควบคุมโดยวิธีเชิงข้อมูลทางสถิติเพื่อประเมินสมรรถนะและความคงทนของระบบควบคุมมุมใบพัดแบบพีไอในระบบกังหันลม โดยศึกษาสองสถานการณ์ที่ส่งผลกระทบต่อสมรรถนะและความคงทนของระบบประกอบด้วยกรณีที่เกิดความเสียหายของอุปกรณ์ควบคุมการทำงานของมุมใบพัดและกรณีที่เกิดความผันผวนของความเร็วลม ข้อมูลการจำลองกระบวนการของสองสถานการณ์ที่ใช้ตัวจำลองกระบวนการฟาสต์เจ็ดในโปรแกรมแมทแลปถูกวิเคราะห์เพื่อที่หาดัชนีสมรรถนะในรูปแบบของดัชนีความแปรปรวนน้อยที่สุดและดัชนีความคงทนโดยการวิเคราะห์การตอบสนองความถี่ ทั้งสมรรถนะและความคงทนถูกประเมินแบบการวัดออนไลน์ ผลแสดงให้เห็นว่าเทคนิคการประเมินสมรรถนะการควบคุมโดยวิธีเชิงข้อมูลทางสถิติสามารถบ่งบอกการเปลี่ยนแปลงสมรรถนะและความคงทนในทั้งสองสถานการณ์ได้อย่างมีประสิทธิผล

จุฬาลงกรณ์มหาวิทยาลัย
Chulalongkorn University

ภาควิชา วิศวกรรมเคมี ลายมือชื่อนิสิต .....

สาขาวิชา วิศวกรรมเคมี ลายมือชื่อ อ.ที่ปรึกษาหลัก .....

ปีการศึกษา 2558

5770380021 : MAJOR CHEMICAL ENGINEERING
KEYWORDS: CONTROL PERFORMANCE ASSESSMENT / MINIMUM VARIANCE INDEX / PI PITCH CONTROL SYSTEM / WIND TURBINE SYSTEM

CHATURAWIT CHINNACHIT: CONTROL PERFORMANCE ASSESSMENT OF WIND TURBINE BY STOCHASTIC METHOD. ADVISOR: ASSOC. PROF. DR.SOORATHEP KHEAWHOM, Ph.D., 68 pp.

This research presents control performance assessment (CPA) techniques by stochastic method to evaluate performance and robustness of PI pitch control system in wind turbine system. Two scenarios affecting performance and robustness of the system, including a fault of pitch actuator and fluctuation of wind speed, are investigated. Simulation data of both scenarios using FAST 7 simulator in MATLAB are analyzed to obtain performance index in terms of minimum variance index and to obtain a robustness index by frequency response analysis. Both performance and robustness are evaluated as on-line measurement. The results showed that CPA techniques by stochastic method adopted in PI pitch control system can effectively indicate variation of performance and robustness in both scenarios.

จุฬาลงกรณ์มหาวิทยาลัย
Chulalongkorn University

Department: Chemical Engineering Student's Signature .....
Field of Study: Chemical Engineering Advisor's Signature .....
Academic Year: 2015

ACKNOWLEDGEMENTS

Firstly, I would like to express kindly my sincere appreciation to my advisor, Associate Professor Dr.Soorathep Kheawhom, who suggests and helps me regarding thesis and education. Moreover, this thesis will not be able to complete absolutely unless there is his guidance.

Next, I also would like to thank my thesis committee members, Professor Dr.Pisan Kittisupakorn, Assistant Professor Dr.Amornchai Arpornwichanop and Dr.Pornchai Bumroongsri for their comments and their time on my thesis. I then like to thank my friends at Computational Process Engineering Research Center for giving me various suggestions and helps.

Finally, I would like to express my sincere gratitude to my parents. Unless my parents support me, I will not have an opportunity to graduate my master's degree.

จุฬาลงกรณ์มหาวิทยาลัย
Chulalongkorn University

CONTENTS

Chulalongkorn University

Page

จุฬาลงกรณ์มหาวิทยาลัย
CHULALONGKORN UNIVERSITY

Page

จุฬาลงกรณ์มหาวิทยาลัย
Chulalongkorn University

LIST OF TABLES

Table **Page**

จุฬาลงกรณ์มหาวิทยาลัย
Chulalongkorn University

LIST OF FIGURES

Figure **Page**

LIST OF FIGURES

Figure **Page**

NOMENCLATURE

R	rotor radius (m)
ρ	air density (kg/m^3)
V	wind speed (m/s)
P_a	aerodynamic power (W)
P_g	generator power (W)
T_a	aerodynamic torque (N·m)
λ	tip speed ratio
β	pitch angle (deg)
$C_P(\lambda,\beta)$	power coefficient
$C_q(\lambda,\beta)$	torque coefficient
ω_r	rotor speed (rad/s)
ω_g	generator speed (rad/s)
ω_s	synchronous speed (rad/s)
ω_{rated}	rated generator speed (rad/s)
T_{em}	generator electromagnetic torque (N·m)
τ_g	generator torque (N·m)
T_{ls}	low speed shaft (N·m)
T_{hs}	high speed shaft (N·m)
J_r	rotor inertia (kg·m2)
J_g	generator inertia (kg·m2)
K_r	rotor external damping (N·m/rad/s)
K_g	generator external damping (N·m/rad/s)
K_{ls}	low speed shaft damping (N·m/rad/s)

จุฬาลงกรณ์มหาวิทยาลัย
Chulalongkorn University

B_{ls}	low speed shaft stiffness (N·m/rad/s)
η_g	generator efficiency (%)
ζ	damping factor
ω_n	natural frequency (rad/s)
K_c	proportional gain
K_I	integral gain
τ_I	integral time
θ	time delay of process
τ_c	design parameter

จุฬาลงกรณ์มหาวิทยาลัย
Chulalongkorn University

Chapter I

Introduction

1.1 Background and motivation

Wind energy is a promising renewable energy that receives increasing attention because it does not contribute to environmental pollution. Moreover, electricity produced from wind energy has a low cost per unit of power (Viveiros et al., 2014). Generally, a variable speed wind turbine system can be effectively used to generate electricity from wind. However, the amount of wind energy depends on geographical conditions and can fluctuate all the time.

Therefore, an effective wind turbine control system is necessary for electricity generation and for equipment protection. The control system generally used consists of a generator torque control, partial load regime, and a pitch angle control, full load regime. The partial load regime is used to maintain optimal rotor speed in order to maximize efficiency. In comparison, the full load regime is employed to keep rotor speed within its allowable limit (Boukhezzar and Siguerdidjane, 2010).

Typically, the control systems of a wind turbine system are designed and tuned during the commissioning stage only. However, the performance of systems gradually deteriorates due to many factors, such as variability of wind speed, wearing of gearboxes and cracking of bearings (Hameed et al., 2009). In order to maintain optimal operation of the systems, control performance assessment (CPA) is required. The basic idea of CPA is a comparison of the performance specified by some benchmark to the current performance of the control system. This comparison yields the performance

Chulalongkorn University

index which is delivered to plant personal in order to detect early performance deterioration.

CPA technology has evolved continuously over the last two decades after Harris first used minimum variance control (MVC) as a benchmark (Harris, 1989). The recent overview of CPA technology and industrial applications presented by (Jelali, 2006) introduces several benchmarks and applications that are used in variously industrial areas, such as refining, petrochemical, chemical sector and pulp & paper plant. In addition, other research works regarding CPA have been presented by many authors e.g. (Jelali, 2007,Carelli and de Souza Jr, 2009, Zhang and Hu, 2012). However, no application of CPA has previously appeared in a control system of a wind turbine.

In this work, CPA techniques are adopted to evaluate the performance and the robustness of the control system in a wind turbine system. A simulation of wind turbine is performed by using FAST 7 code developed by National Renewable Energy Laboratory (NREL) in MATLAB-Simulink. The effects of a faulty pitch actuator and a wind speed fluctuation on the performance of the control system are investigated. In addition, the effect of a faulty pitch actuator and a wind speed fluctuation on the robustness of the control system are also investigated.

จุฬาลงกรณ์มหาวิทยาลัย
CHULALONGKORN UNIVERSITY

1.2 Objective

To investigate the use of CPA techniques in wind turbine system.

1.3 Scopes of work

1. Wind turbine simulation is performed by using FAST 7 code developed by National Renewable Energy Laboratory (NREL) in MATLAB-Simulink.

2. Characteristics of AWT27 wind turbine is used in this work

3. Wind speed is assumed in a range of 10 to 15 m/s

4. Pitch control system is regulated by PI controller and torque control system is modelled as induction generator.

5. Effects of a faulty pitch actuator and a wind speed fluctuation on the performance of the control system are investigated.

6. Effects of a faulty pitch actuator and a wind speed fluctuation on the robustness of the control system are also investigated.

จุฬาลงกรณ์มหาวิทยาลัย
Chulalongkorn University

1.4 Organization of thesis

Chapter II reviews an overview of research regarding control performance assessment technology (CPA), stability analysis and various faults and control strategy in wind turbine.

Chapter III presents theories regarding principle of wind turbine, principle of control performance assessment, wind turbine modeling and PID controller and SIMC tuning rules.

Chapter IV describes wind turbine simulation, control regimes, two faulty scenarios and procedures of CPA and robustness assessment.

Chapter V introduces the results regarding effects of a faulty pitch actuator and a wind speed fluctuation on the performance of the PI pitch control system and effects of a faulty pitch actuator and a wind speed fluctuation on the robustness of the PI pitch control system.

Chapter VI gives conclusion and recommendation regarding the use of CPA techniques in wind turbine system.

จุฬาลงกรณ์มหาวิทยาลัย
CHULALONGKORN UNIVERSITY

Chapter II

Literature reviews

In this chapter, an overview of research regarding control performance assessment technology (CPA), stability analysis and various faults and control strategy in wind turbine will be presented. Moreover, these works will provide many ideas to apply in this work.

2.1 CPA methods

Various techniques for CPA have been introduced over the last two decades. The method of CPA first proposed by (Harris, 1989) is performance evaluation that compares output variance of closed loop system to minimum variance benchmark (MV). This comparison provides performance index that directly relates to the performance of process, the quality of product and energy or material consumption. After that, MV benchmark is extended to generalized minimum variance benchmark that considers control action penalization, suggested by (Grimble, 2002).

Chulalongkorn University

Besides MV benchmark used for performance evaluation in linear control system, many researchers have introduced various benchmarks that used for performance evaluation in advance control system, linear quadratic Gaussian benchmark (LQG) and model predictive control benchmark (MPC). The LQG benchmark proposed by (Huang and Shah, 1999) provides performance bound in term of the weighted input and output. For the MPC benchmark recommended by (Patwardhan et al., 1998), this benchmark used for the performance evaluation of MPC controller that compares actual design objective to achieved performance.

2.2 Stability analysis

The concept of stability analysis is a metric that indicates the robustness of the control system. This metric involves with the sensitivity of control system to process variations and to uncertainty in the process model. For research involving in robustness analysis is introduced by (Garpinger et al., 2014). Their research presented trade-off plots to analyze the robustness for different three processes regulated by PI and PID controller. Their robustness analysis used sensitivity functions as criterion. By factors studied is various controller parameters and different tuning methods resulting in the robustness of control system. From their studies, the result showed that the trade-off plots of the robustness provide level curves of the robustness as functions of proportional and integral gain. Therefore, the trade-off plots are useful to indicate the robustness about controller tuning.

Besides the research introduced by (Garpinger et al., 2014), there is a study that involves with using maximum sensitivity in analysis of the robustness degree of the control system presented by (Jin et al., 2013). Their study presented robust tuning for internal model controller can help enhance the robustness of the control system. The robustness degree of control system based on maximum sensitivity is compared to the parameters of controller in order to give a clear design criterion to IMC controller. Their result showed that the comparisons between robustness degree and the parameter of controller are easy to design the IMC controller and can choose the robustness degree.

2.3 CPA adopted in the processes

In order to maintain the quality of product and reduce material and energy consumption in industry. Metal industry takes CPA to use in metal processing (Jelali, 2007). Their study presented performance assessment of two case studies in the control system of a tandem cold rolling mill, a feedforward/feedback strip thickness controller and an internal model control of the strip flatness. The performance of the control system is investigated from routine operating data and measured by using minimum variance benchmark. After they used CPA to evaluate the performance, their results showed that the performance of the flatness controller is satisfactory, thus it is not essential to retune controller. However, feedback thickness controller indicated poor performance, thus re-tuning is required. From their studies, it can be concluded CPA performs well and can resolve performance problem in the metal process.

Besides metal processing, there are studies of CPA that applying to simulation of control system of water level in steam generator and hydrotreater reactor. For the study of the control system of water level in steam generator (Zhang and Hu, 2012). It is necessary to keep and monitor always the control system of water level in steam generator because it is main device of nuclear power plant. Their study focused on adopted CPA in two PI controller in term of minimum variance index due to no application in this field. Their result showed that CPA can be effectively used in this field. Moreover, they suggested that future work is more interesting in adopting with nuclear power industry.

In research of hydrotreater reactor (Carelli and de Souza Jr, 2009), CPA is used to compare the performance of different controller design, PID controller and MPC

controller because hydrotreating process is a key part in petroleum refinery. Furthermore, it can produce pollution to environment due to ineffectiveness in control system. Therefore, in their work, CPA is necessary to analyze the different controller design. Their benchmark used is minimum variance control. Their result showed that MPC is better than PID in aspect of deterministic and stochastic performances. From their research, it can be concluded that CPA is useful to detect the performance of different controller design. In addition, it can help decide proper controller implemented in the processes.

2.4 Control strategies of wind turbine

Reliable control strategies can help wind turbine reach maximum performance. Multivariable control strategy for variable speed wind turbine has been proposed by (Boukhezzar et al., 2007). This control strategy is combination a nonlinear dynamic state feedback torque control with a linear controller of blade pitch angle. The operations of this control strategy can be divided into two regimes, above-rated wind speed and below-rated wind speed. At below-rated wind speed, wind turbine will be operated at inconstant rotor speed in order to maximum energy from wind. Torque control is used as control input for varying rotor speed and pitch angle is fixed. For above-rated wind speed, the rotor speed is kept at its nominal speed. The torque control is constant and pitch angle is adjusted to shed unwanted wind. In their studies, multivariable control strategy is compared with other control strategies, PID and LQG controller. Their result showed that the proposed control strategy can achieve good performance in rotor speed and electrical power regulation.

2.5 Faults occurring in wind turbine

2.2.1 Faulty pitch systems

In pitch systems, there are two types that are used in the wind turbine, electric motor drive and hydraulic drive. However, the hydraulic drive is mostly used in the pitch system. The fault mainly found in hydraulic pitch system is oil leakage. Moreover, faulty control system found in pitch control is pitch angle faults, overheated motor and signal malfunctions. The overheated motor fault results from oil leakage in the gearbox and the signal malfunctions can result in runaway wind turbine(Chen et al., 2013). In part of pitch angle faults, the lack of lubricant can lead to damages of various components, such as pitch bearings, pitch gears and pitch encoders(Kusiak and Verma, 2011).

2.2.2 Faulty gearbox

Modern wind turbine mainly uses gearbox in order to change low rotational speed into high rotational speed. However, fault of gearbox regularly occurs in wind turbine due to intermittence of wind speed (Nejad et al., 2014). Mainly, cracking of bearing befalls on bearing balls and bearing raceways. These problems result from inadequate lubricant and overload. Furthermore, ball corrosion may occur on the gearbox because the use of different lubricant will react chemically then lead to corrosion.

2.2.3 Faulty generator

Fault of electrical generator in wind turbine comes from two causes, mechanical fault and electrical fault. The electrical fault consists of stator winding fault and rotor winding fault. However, the main fault of electrical generator is short circuits that lead

จุฬาลงกรณ์มหาวิทยาลัย
Chulalongkorn University

to tri-phase asymmetry. In addition, there are many factors that produce the short circuits, such as insulation damage of conductive part, operating the disconnector switches with load, power on prior to the demolition of the old cables after inspection, and natural phenomena such as wind, rain and snow(Attya and Hartkopf, 2012). For mechanical fault, it is mainly rotor fault and bearing fault. Rotor fault results from unbalanced rotor, cracking of rotor and loosening socket. On the other hand, bearing fault occurs due to instability of oil film.

จุฬาลงกรณ์มหาวิทยาลัย
Chulalongkorn University

Chapter III

Theory

3.1 Principle of wind turbine

Wind turbine is a complex electromechanical device that can convert kinetic energy in the wind into mechanical energy. After that, mechanical energy can be directly used by machinery, for example, windmill is used to mill grain or pump water. On the other hand, it can be also changed into electricity by generator.

3.1.1 Aerodynamic lift and aerodynamic drag wind turbine

Mainly, wind energy conversion system can be divided into two different types. Those depend on aerodynamic drag and aerodynamic lift. Lift and drag is the forces rotating the blades of wind turbine. Aerodynamic drag is used to rotate the rotor of vertical-axis wind turbine. On the other hand, Aerodynamic lift is used to rotate the rotor of horizontal-axis wind turbine. Drag force to move the blades of the wind turbine is not commonly used because of poor power extraction from the wind. Therefore, most of modern wind turbines are mostly based on the aerodynamic lift.

3.1.2 Types of wind turbine

Wind turbine is generally classified into two types, horizontal-axis and vertical-axis. In the 1920s, vertical-axis wind turbine originated by French engineer uses vertical symmetrical airfoils. The vertical-axis wind turbine has curve blades connected at the top and at the bottom and rotates perpendicularly with ground level, as illustrated in Figure 3.1. The advantage of this type is that it can operate independently of the wind

direction and heavy gearbox and generator can be installed at ground level. However, it still has disadvantage that is noise pollution.

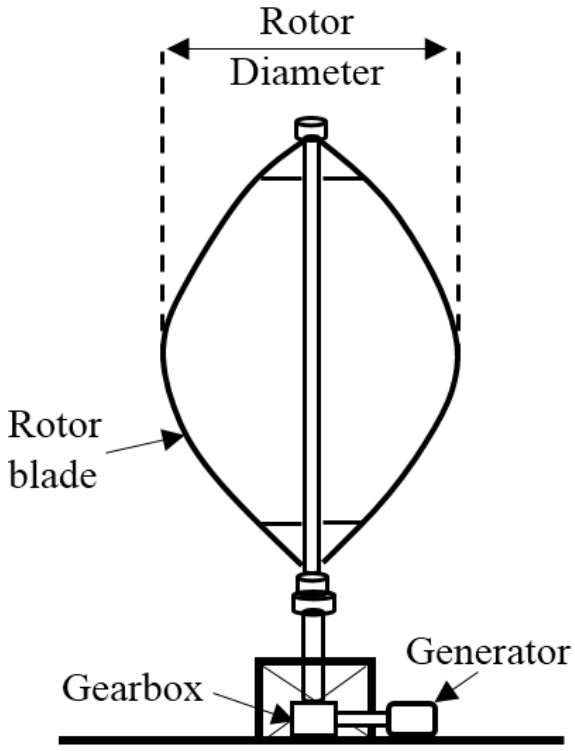

Figure 3.1 Vertical-axis wind turbine schematic

For horizontal-axis wind turbine, it has received much attention in the application of wind turbine. A horizontal-axis wind turbine mainly consists of a tower, a rotor and a nacelle that is located at the top of a tower, as shown in Figure 3.2. The rotor has two types, three rotor blades and two rotor blades. For two rotor blades, it has the advantage that the tower top weight is lighter and the all supporting structure can be built lighter. However, three rotor blades have the advantage that the rotor moment of inertia is better to handle than the rotor moment of inertia of two rotor blades. Moreover, three rotor blades are better visual aesthetics and a lower noise level than two rotor blades(Ackermann and Söder, 2000).

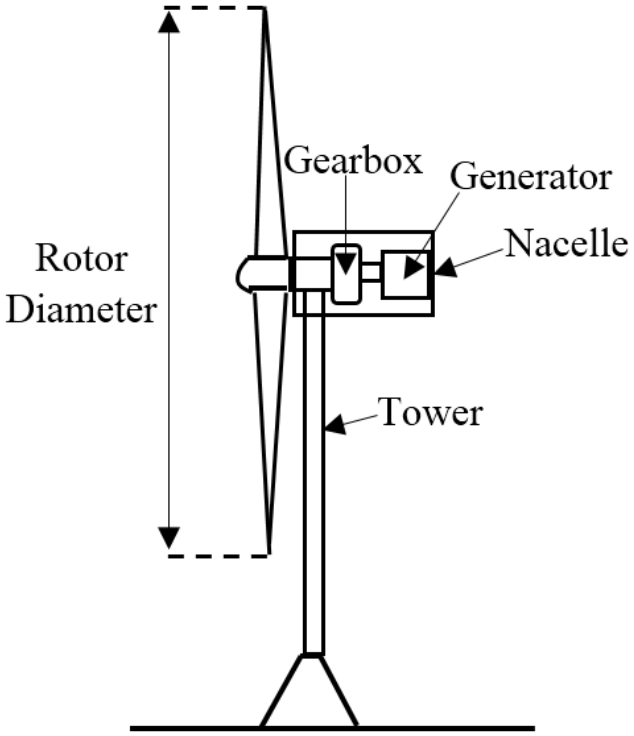

Figure 3.2 Horizontal-axis wind turbine schematic

3.1.3 Main components of modern wind turbine

Presently, modern wind turbine mainly consists of tower, nacelle and rotor. The rotor can be divided into two parts, blades and hub. In part of nacelle, it is a room in which contains key components of wind turbine, such as gearbox, electrical generator, mechanical brake and control system. The gearbox is a heavy device which can help increase the rotational speed to drive electrical generator. For the electrical generator, it is employed to convert the mechanical energy into electrical energy. For equipment protection, the mechanical brake is used to stop operation of wind turbine in case of higher wind speed. The control system can help wind turbine to produce electricity effectively and also reduce equipment damage. The main components of modern wind turbine are shown in Figure 3.3.

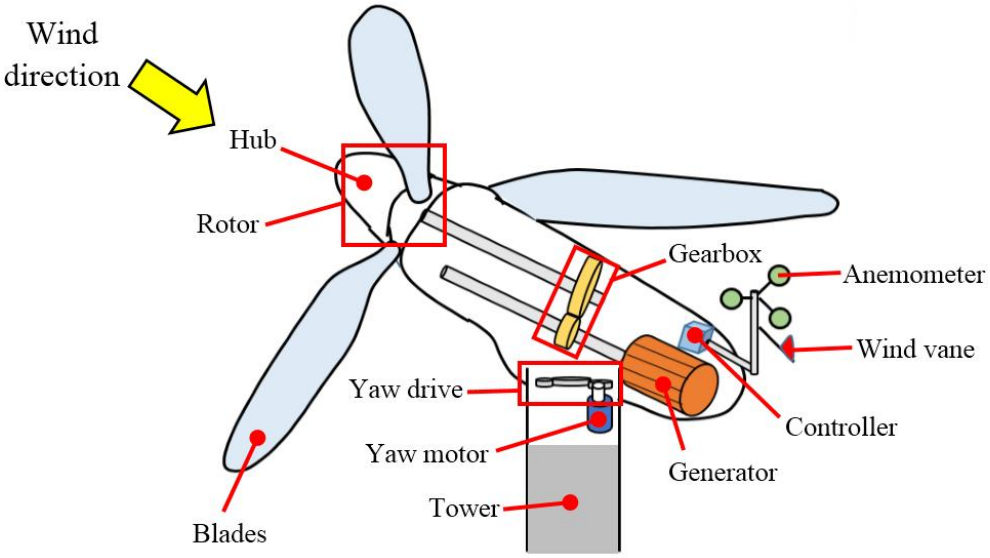

Figure 3.3 The main components of modern wind turbine

3.1.4 Control regimes of modern wind turbine

Generally, it can be divided into three methods, torque control, pitch control and yaw control. Torque control is used to maintain optimal rotor speed in order to maximize efficiency. However, at high wind speed or above 12 m/s, torque control cannot regulate because it has its limitation. Therefore, pitch control is needed to assist torque control by regulating the output power of the wind turbine and also by keeping the rotor speed within its allowable limit. In addition, the angle of rotor blades is manipulated by pitch control in case of high wind speed in order to shed the unwanted power from the wind. For yaw control, it is used for rotating the nacelle to confront with the wind direction measured by a wind wane.

3.1.5 Wind power calculation

The power in the wind is the total available energy per unit. The power in the wind is converted into the mechanical energy of the rotor. However, wind turbine cannot extract the power in the wind completely. This means that it can convert the power in the wind that supplying to its rotor area only. Therefore, in order to calculate maximum power that can be harnessed from the wind, the Betz's law is required.

Wind energy is the kinetic energy of moving air:

$$E_{kinetic} = \frac{1}{2}mv^2 \tag{1}$$

Where m is the mass of the moving air (kg) and v is the velocity (m/s^2)

However, the mass can be define as:

$$m = \rho V \tag{2}$$

Where ρ is the air density (kg/m^3) and V is the volume of the air

Equation (2) is substituted into Equation (1) to become Equation (3)

$$E_{kinetic} = \frac{1}{2}\rho V v^2 \tag{3}$$

By definition, power is energy divided by time. Equation (4) shows then the wind power:

$$P_{wind} = \frac{E_{kinetic}}{\Delta t} = \frac{1}{2}\frac{\rho V v^2}{\Delta t} \tag{4}$$

The volume of the air is distance multiplied with capture area:

$$V = Av\Delta t \tag{5}$$

Equation (5) is substituted into Equation (4) to become Equation (6)

$$P_{wind} = \frac{1}{2}\rho A v^3 \tag{6}$$

From Equation (6), it can be implied that the wind power involves in the wind passing through the capture area. When wind speed increases double, it will give eight times the wind power. However, the ideal power is reduced by two inefficient situation, gearbox losses and generator efficiency. Therefore, the value of the actual power is limited by Betz coefficient (Cp = 0.59). The actual wind power is then;

$$P_{wind} = \frac{1}{2}C_p\rho A v^3 \tag{7}$$

Equation (7) shows the theoretical maximum power in the wind which can be extracted by wind turbine.

จุฬาลงกรณ์มหาวิทยาลัย
Chulalongkorn University

3.2 Principle of control performance assessment (CPA)

This section describes CPA to evaluate the performance of control system. The basic idea of CPA is a comparison of the performance specified by some benchmark to the current performance of the control system. This yields the performance index which is delivered to plant personal in order to detect early performance deterioration. Before discussing regarding CPA, It is necessary to know basic theory of control system and root causes of control problem.

3.2.1 Basic theory of control system

A control system is a connected components that consist of controller, actuator, sensor and process. The configuration of the control system, as shown in Figure 3.4, has main objective to control the behavior of the process in a desirable way.

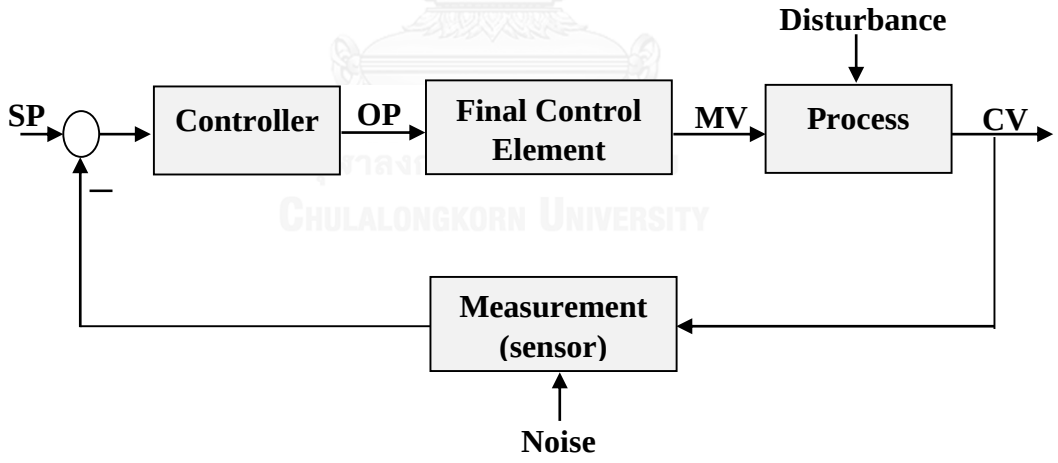

Figure 3.4 Block diagram of closed-loop system

From Figure 3.4, control variable (CV) of process will be controlled. The controller is used to keep CV at set-point (SP) while disturbance is coming in the process. Final control element receives the controller output (OP) in order to manipulate then the process. If all components of the control system work properly, the control system will

achieve good process control. Therefore, before tuning a closed-loop control system, it is important to investigate that each component and design are suitable.

3.2.2 Root causes of control problem

Generally, the control system will perform well at the commissioning stage. After that, the performance of the control system gradually deteriorate all the time. As reported by (Hoo et al., 2003), around 60 % of controllers in industry have problems. These problems arise from various key factors, such as inadequate controller tuning, equipment damage and inappropriate control structure. Inadequate controller tuning is that the controller is tuned bases on a poor model or improper controller types is used. Almost 90 % of controller installed in industry are PID controller. Although, other controllers are more suitable.

For equipment damage, it is one of reasons that restricts the control system to achieve control performance target. Thus, all components of control loop must be healthy in order to avoid cause of poor control performance. Poor control performance results from malfunction of devices, sensors and actuators. By reasons mentioned, re-tuning controller cannot overwhelm poor control performance. It is important to inspect the properties of control loop, e.g., signal levels, noise levels, non-linearity and equipment conditions. In part of inappropriate control structure, it mainly involves with insufficient degree of freedom, lack of time-delay compensation, inadequate pairing of input and output and the presence of strong non-linarites.

3.2.3 CPA based on minimum variance benchmark

This section will present description of the control system in term of discrete time system because of the CPA using discrete time system in evaluation. The discrete time system of feedback control system is shown in Figure 3.5.

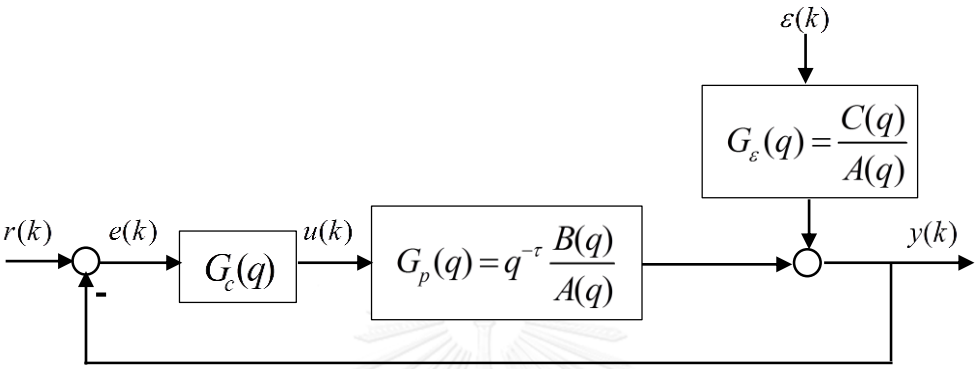

Figure 3.5 Structure of feedback control system

Where $r(k)$ is set-point, $u(k)$ is controller output, $y(k)$ is process output $\varepsilon(k)$ is unmeasured disturbance and $e(k)$ is control error. G_c, G_p and G_ε are the transfer functions of controller, process and disturbance respectively. The set-point is set to zero by convenience and the disturbance are assumed to be zero mean.

The control system shown in Figure 3.5 can be described by autoregressive–moving-average model with exogenous inputs model (ARMAX model):

$$y(k) = q^{-\tau}\frac{B(q)}{A(q)}u(k) + \frac{C(q)}{A(q)}\varepsilon(k) \tag{8}$$

Where $\varepsilon(k)$ is a zero-mean white noise with the variance σ_ε^2. τ is a the dynamics that contain a delay of τ samples. $A(q)$, $B(q)$ and $C(q)$ are polynomials in q^{-1} of order n, m and p respectively:

$$\begin{aligned} A(q) &= 1 + a_1 q^{-1} + a_2 q^{-2} + ... + a_n q^{-n} \\ B(q) &= b_0 + b_1 q^{-1} + b_2 q^{-2} + ... + b_m q^{-m} \\ C(q) &= 1 + C_1 q^{-1} + C_2 q^{-2} + ... + C_p q^{-p} \end{aligned} \tag{9}$$

The term of B is non-zero constant because the input u does not affect promptly the output. For example, there is at least one sample delay ($\tau \geq 1$). The polynomials A and C are monic because their term is unity. Note that the system identification in term of polynomial operator form is used in thesis for the description of input and output model. The forward operator denoted by q has the property.

$$qf(k) = f(k+1) \tag{10}$$

Where $(k+1)$ is the next sampling instance. Similarly, the backward shift operator q^{-1} is define as:

$$q^{-1} f(k) = f(k-1) \tag{11}$$

Where $(k+1)$ is the previous sampling instance.

For example, the difference equation of a linear system is given:

$$y(k) + a_1 y(k-1) + ... + a_n y(k-n) = b_0 u(k) + b_1 u(k-1) + ... + b_m u(k-m) \tag{12}$$

Equation 12 will thus become:

$$(1 + a_1 q^{-1} + ... + a_n q^{-n}) y(k) = (b_0 + b_1 q^{-1} + ... + b_m q^{-m}) u(k) \tag{13}$$

Equation 13 can be simplified by:

$$A(q) y(k) = B(q) u(k) \tag{14}$$

For control performance assessment, it will be described as following steps. Collecting data from the closed-loop system then choose the time-series model types and order. AR and ARMAX types is typically used:

$$y(k) = \frac{C(q)}{A(q)}\varepsilon(k) \tag{15}$$

From Equation 14, it will become impulse-response of the time-series model:

$$y(k) = \left(\sum_{i=1}^{\infty} e_i q^{-1}\right)\varepsilon(k)$$

$$y(k) = \left(e_0 + \underbrace{e_1 q^{-1} + e_2 q^{-2} + ... + e_{\tau-1} q^{-(\tau+1)}}_{\text{feedback-invarint}}\right)\varepsilon(k) + \left(\underbrace{e_\tau q^{-\tau} + e_{\tau+1} q^{-(\tau+1)} + ...}_{\text{feedback-varing}}\right)\varepsilon(k) \tag{16}$$

The impulse-response coefficients shown in equation 15 can be estimated via polynomial long division. The feedback-invarint terms are not a function of the process model and the controller but they depend on the characteristics of disturbance coming to the process. Thus, the minimum variance estimated corresponds to a part of feedback-invariant, as given by:

$$\sigma_{MV}^2 = \sum_{i=0}^{\tau-1} e_i^2 \sigma_\varepsilon^2 \tag{17}$$

Normally, the first coefficient of the impulse response (e_0) is equal to unity.

The estimation of actual output variance can be directly estimated from the collected output samples using the standard relation, as given by:

$$\sigma_y^2 = \frac{1}{N-1}\sum_{k=1}^{N}(y(k) - \bar{y})^2$$
$$\bar{y} = \frac{1}{N}\sum_{k=1}^{N} y(k) \tag{18}$$

However, it is suggested to use only the estimated time-series model for evaluation of the actual variance. From the impulse-response of the time-series model, it can be calculated by:

$$\sigma_y^2 = \sum_{i=0}^{\infty} e_i^2 \sigma_\varepsilon^2 \tag{19}$$

จุฬาลงกรณ์มหาวิทยาลัย
Chulalongkorn University

The performance index (η_{MV}) corresponds to the ratio of variance that can theoretically be achieved under minimum variance control. η_{MV} lies in 0 to 1. 0 indicates poor performance and 1 indicates good performance. The performance index (η_{MV}) can be calculated by:

$$\eta_{MV} = \frac{\sigma_{MV}^2}{\sigma_y^2} \tag{20}$$

3.2.4 Selection of sampling time

Generally, the closed loop data of control system used for CPA must be collected at the sampling time of controller. However, in practice, it is recommended to lessen properly the closed loop data in order to reduce computational time. Moreover, the selection of the sampling time interval and the number of orders in model are not independent of one another because they affect the total time span captured by the autoregressive terms. The method of sampling time selection proposed by (Thornhill NF, 1999) is to choose the order of the AR model that is equal to 30 for all types of the control system and then adjust the sampling time interval individually for each control system. The suggestion is to select the sampling interval such that a typical closed loop impulse response is fully captured within 30 samples. An example of effects of sampling time on the impulse response is shown in Figure 3.6. The data are from a thickness control loop in a cold rolling mill(Jelali, 2007). From the effects of sampling time, it is important to avoid both over-sampling and under-sampling. If the closed loop data are sampled too frequently, the transient part of the closed loop impulse response will not settle within 30 samples. On the other hand, if the closed loop data are under-sampled, the closed loop impulse response will settle within a few samples and is not

adequately captured because interesting features may be missed between samples. As aforementioned example, an suitable sampling time must be selected in a range of 100 ms to 50 ms in order to avoid both over-sampling and under-sampling.

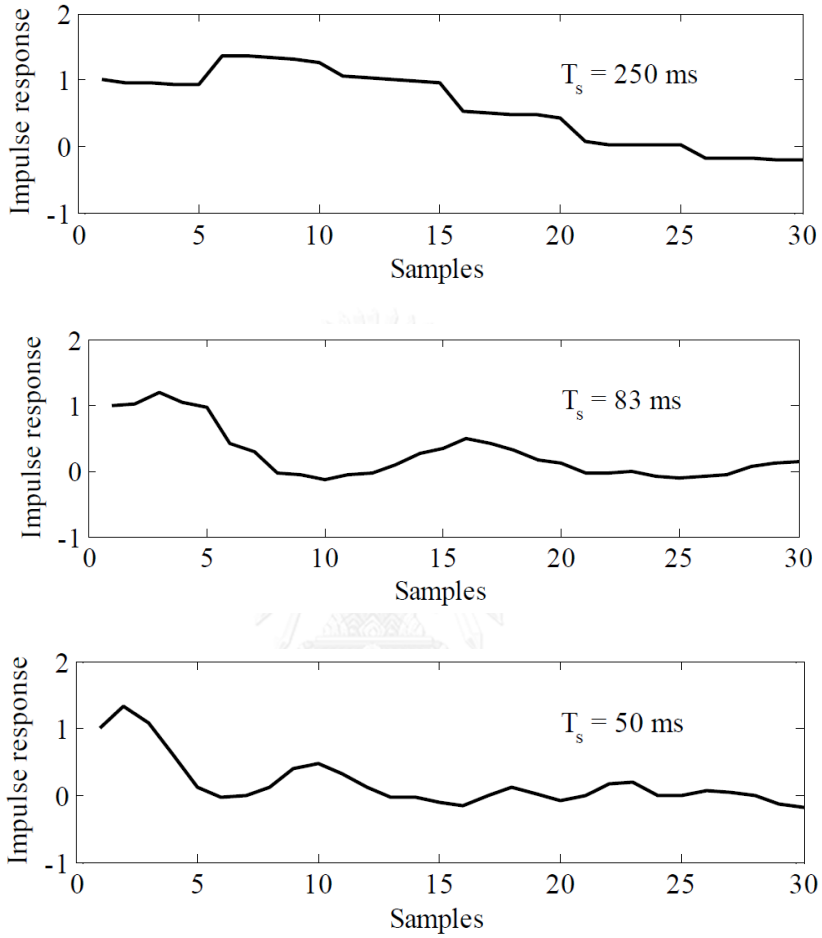

Figure 3.6 Effects of sampling time on the impulse response

3.2.5 Selection of data length

The data length used for CPA clearly results in the statistical confidence in the performance index value because data length increases, it will affect to increase the statistical confidence as well. When data of the control error are considered, it is not necessary for the control system to stay at the same set-point throughout the period of data recording, but it is desirable that the characteristics of the control system remain

unchanged. Data episodes during instrument recalibration episode or known plant disturbances like feed switches or partial trip have to be avoided.

The effect of data length can be assessed by using the confidence limits given by(Desborough and Harris, 1992):

$$\sigma_{\hat{\eta}}^2 \approx \frac{4}{N}(1-\hat{\eta})\left(\sum_{k=1}^{\tau-1}\left[\rho_y(k)-\rho_\varepsilon(k)\right]^2+\sum_{k=1}^{\infty}\left[\rho_y(k)\right]^2\right) \tag{21}$$

From equation 21, short data segments will increase the standard deviation of the statistical estimation. Whereas, long data segments lead to lower the standard deviation. However, the sets of too long data provide misleading results when many different response characteristics are juxtaposed into a set of long data. It is agreed by many researchers that a good balance between statistical confidence and the steady state of the characteristics of the control system is accomplished with the data length from 1000 to 2000 samples. The suggestion of data length is 1500 samples.

As an example of measured data from a strip-thickness control system will be shown the effects of data length N. Figure 3.7 shows the time trend of control error from a strip-thickness control loop for 2334 samples. When all data points are used, the Harris index is 0.724 with a standard deviation of 0.101. The four plots in Figure 3.8 indicate the index values and the standard deviation when shorter data collected are used. For example, in the lower right hand plot the collected data are 300 points each ($(\sigma = 0.102 - 0.406)$. They have considerable variability and the error bars, which represent the standard deviation, are significantly large. Whereas, the standard deviations for collected data of 1500 points are quite smaller $(\sigma = 0.102)$. Particularly in the plots of $N = 300$ at disturbances between the samples 1020 and 1150 and the

samples between 1550 and 1675, it can be clearly seen that shorter sequence are more responsive to change in the characteristics of the control system.

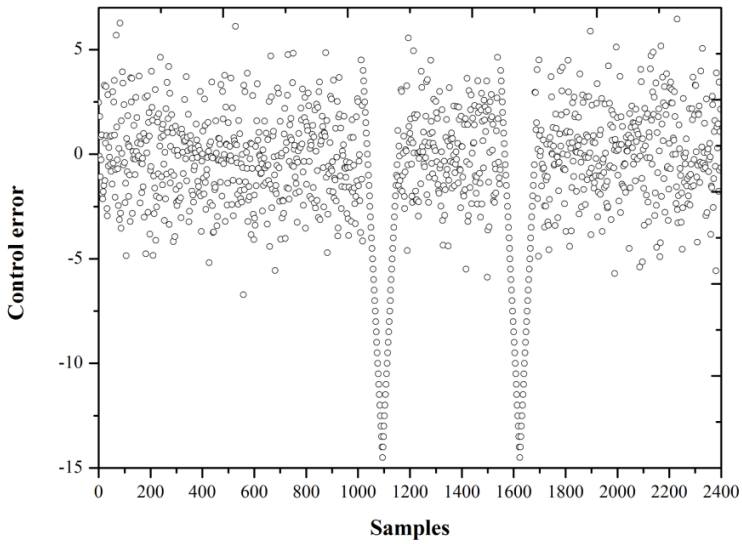

Figure 3.7 The control error of a strip-thickness control loop

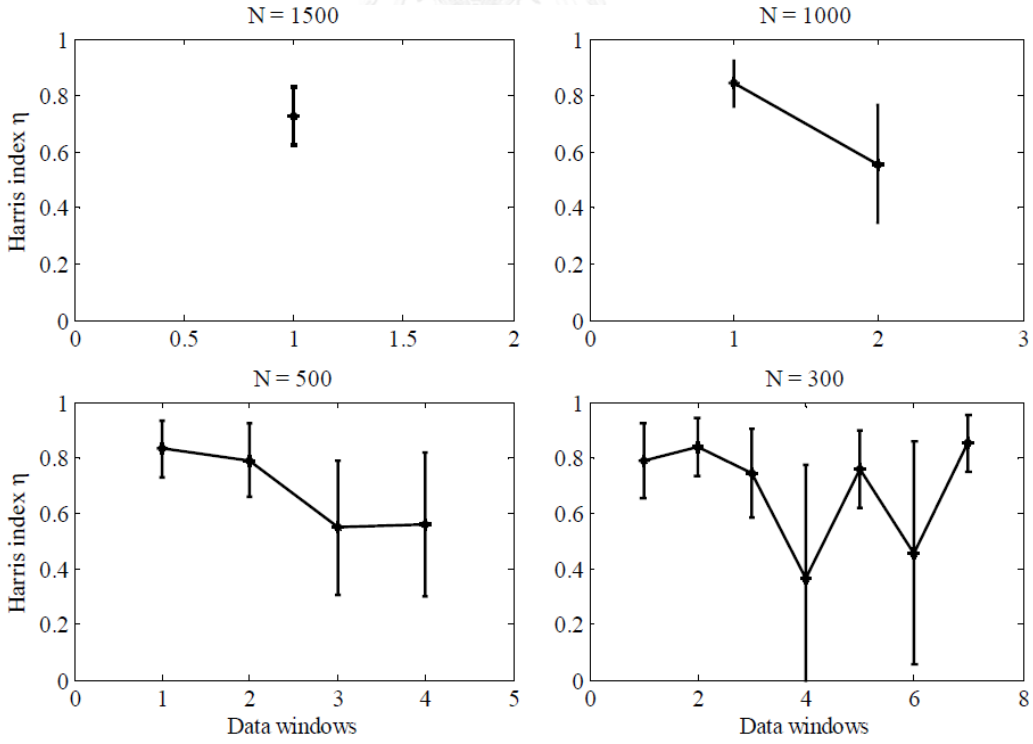

Figure 3.8 Effects of data length on the standard deviation of Harris index.

3.2.6 Selection of model order

In selection of model order, it significantly results in the estimated performance index values. For time-varying closed loop systems, the proper model order must be determined for each individual data segment. Various disturbances coming in the system will change the model order of the closed loop system. Therefore, the various suggestion to select model order proposed by many researchers will be presented. Firstly, (Desborough and Harris, 1992) introduced to start with some small model order like $n = 5$ and gradually increase model order n until the performance index will not change. Next, (Thornhill NF, 1999) used a fixed 30th-order AR model and adjust the sampling time such that the closed loop impulse response is fully captured within 30 samples. After that, (Horch, 2000) found that a suitable model order for AR model is in range of 15 and 25. Eventually, (Goradia et al., 2005) suggested to use 20th-order plus the time delay of process.

3.2.7 Stability and robustness analysis based on sensitivity function

This section presents the stability and robustness analysis based on sensitivity function(Garpinger et al., 2014). The concept of frequency analysis is important to stability and robustness analysis. This metric can indicate that when the control system will face with instability. Considering block diagram of a feedback control system is shown in Figure 3.9.

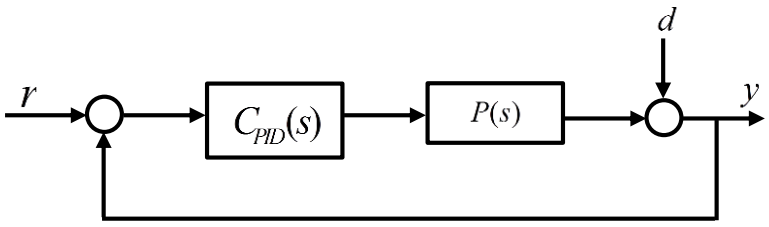

Figure 3.9 Block diagram of a feedback control system

Where $C_{PID}(s)$ is PID controller and $P(s)$ is the transfer function of process

The PID controller is given by:

$$C_{PID}(s) = k_p\left(1+\frac{1}{\tau_I s}+\tau_d s\right) \tag{22}$$

From Figure 3.9, the loop transfer functions can be written by:

$$G_{loop} = C_{PID}(s)P(s) \tag{23}$$

s in equation 23 is substituted by $j\omega$, it will become:

$$G_{loop} = C_{PID}(j\omega)P(j\omega) \tag{24}$$

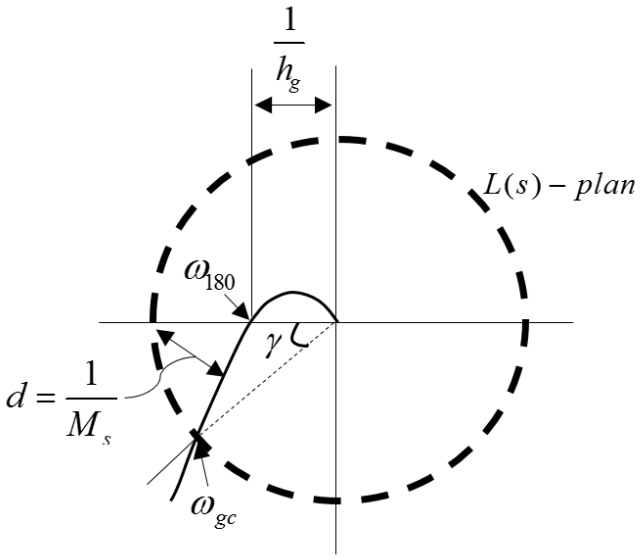

Figure 3.10 Nyquist curve of the loop transfer function with gain, phase and stability

The stability and robustness of the control system based on maximum value of the sensitivity function can be calculated by:

$$M_{st} = \max_{\omega}(|S(j\omega|,|T(j\omega|),\ \forall\omega\in\mathbb{R} \tag{25}$$

Where $$S(j\omega) = \frac{1}{1 + G_{loop}(j\omega)} \tag{26}$$

$$T(j\omega) = \frac{G_{loop}(j\omega)}{1 + G_{loop}(j\omega)} \tag{27}$$

Noted that d is the shortest distance of the Nyquist curve of the loop transfer function to the critical point, as shown in Figure 3.10.

Proper values of M_{st} are in range of 1.2 to 2.0. Values close to 1.2 are more conservative and values close to 2 are more aggressive controllers. The values of M_{st} relates to the gain margin and phase margin as following:

$$h_g > \frac{M_{st}}{M_{st} - 1},\ \gamma > 2 \cdot \sin^{-1}\left(\frac{1}{2 \cdot M_{st}}\right) \tag{28}$$

where h_g is the gain margin and γ is the phase margin

จุฬาลงกรณ์มหาวิทยาลัย
Chulalongkorn University

3.3 Wind turbine modeling

3.3.1 FAST 7 Simulator

FAST 7 developed by National Renewable Energy Laboratory (NREL) is used as wind turbine simulator in MATLAB-Simulink(Singh et al., 2014). Moreover, this simulator is widely used as validation for many researches in the development of new control systems of wind turbines and has been accepted by the scientific community. FAST 7 is an appropriate simulator to design and analyze the control system of wind turbine, as shown in Figure 3.11.

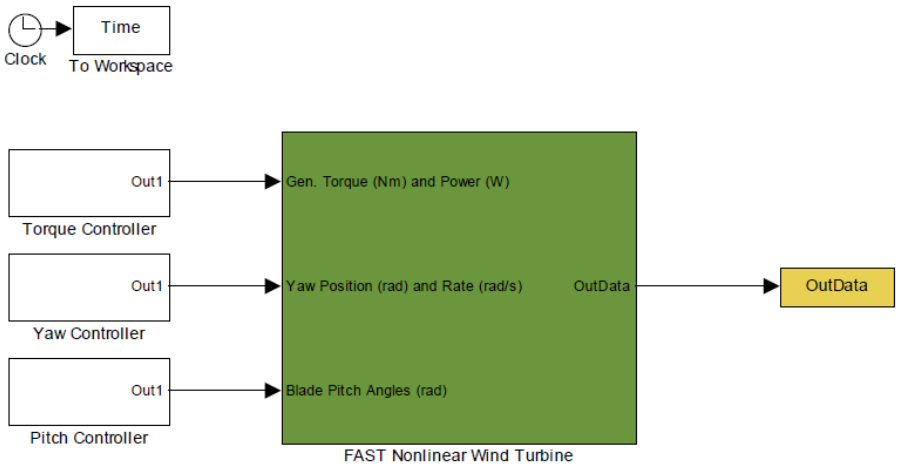

Chulalongkorn University

Figure 3.11 FAST 7 simulator in MATLAB-Simulink

Moreover, mathematical modeling of FAST 7 simulator in MATLAB-Simulink is non-linear model. Thus, mathematical modeling of wind turbine presented by (Boukhezzar et al., 2007) will be introduced because their mathematical modeling corresponds to FAST 7 simulator from validation.

3.3.2 Mathematical modeling of wind turbine

Generally, a variable-speed wind turbine composes of an aero-turbine, a gearbox and a generator. The aerodynamic power captured by the rotor is given by:

$$p_a = \frac{1}{2}\rho\pi R^2 C_p(\lambda,\beta)v^3 \tag{29}$$

Where R is the rotor radius, ρ is the air density, v is the wind speed and C_p is the power coefficient. The power coefficient depends on blade pitch angle (β) and the tip-speed ratio (λ), which are defined as following:

$$\lambda = \frac{\omega_r R}{v} \tag{30}$$

From equation 30, it can be seen that if the rotor speed or wind speed changes, the tip-speed ratio will be induced. The change of tip-speed ratio leads to power coefficient variation. The aerodynamic torque coefficient will relate to the power coefficient by using the relationship:

$$P_a = \omega_r T_a \tag{31}$$

Equation 29 is substituted into Equation 31, the aerodynamic torque coefficient will become:

$$T_a = \frac{1}{2}\rho\pi R^3 C_q(\lambda,\beta)v^2 \tag{32}$$

จุฬาลงกรณ์มหาวิทยาลัย
Chulalongkorn University

Where

$$C_q(\lambda,\beta) = \frac{C_p(\lambda,\beta)}{\lambda} \tag{33}$$

Power and torque coefficient curves as a function of pitch angle and tip-speed ratio are shown in Figure 3.12. Note that these curves are not the same in each wind turbine.

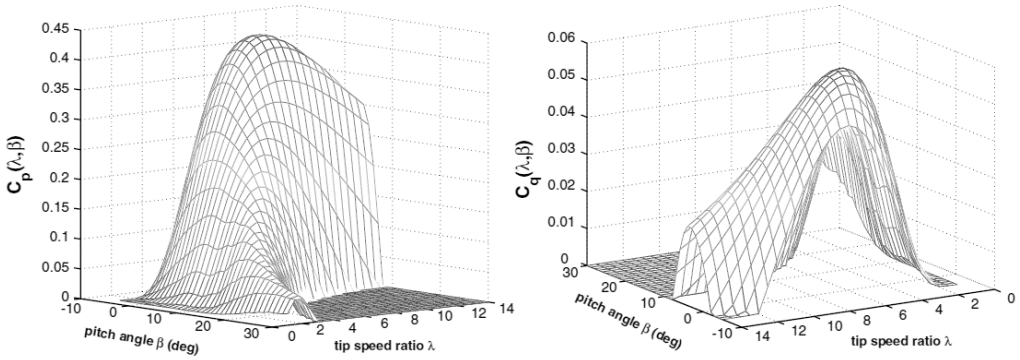

Figure 3.12 Power and torque coefficient curves (Boukhezzar et al., 2007)

A two-mass model of the wind turbine is shown in Figure 3.13.

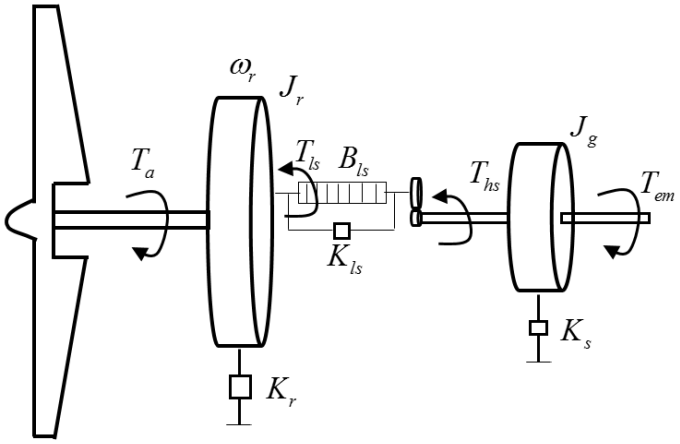

Figure 3.13 Two-mass model of the wind turbine (Boukhezzar et al., 2007)

The dynamic response of the rotor driven at a rotor speed ω_r by the aerodynamic torque T_a is given by:

$$J_r\dot{\omega}_r = T_a - T_{Is} - K_r\omega_r \tag{34}$$

Where J_r is the rotor inertia, T_{Is} is the low-speed shaft torque and ω_r is the rotor speed The low-speed shaft torque acts as braking torque on the rotor. The difference between the rotor speed and low-speed shaft results in the torsion and friction effects, as given by:

$$T_{Is} = B_{Is}(\theta_r - \theta_{Is}) + K_{Is}(\omega_r - \omega_{Is}) \tag{35}$$

Where B_{Is} is the low speed shaft stiffness, K_{Is} is the low speed shaft damping and ω_{Is} is the low-speed shaft

The generator is driven by the high-speed shaft torque and braked by the generator electromagnetic torque:

$$J_g \dot{\omega}_g = T_{hs} - K_g \omega_g - T_{em} \tag{36}$$

Where T_{hs} is the high-speed shaft torque and T_{em} is the electromagnetic torque

The gearbox ratio is given by:

$$n_g = \frac{T_{Is}}{T_{hs}} = \frac{\omega_g}{\omega_{Is}} \tag{37}$$

จุฬาลงกรณ์มหาวิทยาลัย
Chulalongkorn University

3.4 PID controller and SIMC tuning rules

3.4.1 PID controller

A proportional-integral-derivative controller or PID controller is a general controller which is commonly used in modern industries. A PID controller continuously calculates an error value as the difference between a desired set-point and a measured control variable. The controller attempts to minimize the error value all the time by adjustment of a controlled variable, such as the position of control value, a damper, or the power supplied to a heating devices. A block diagram of a PID controller in feedback control system is showed in Figure 3.14.

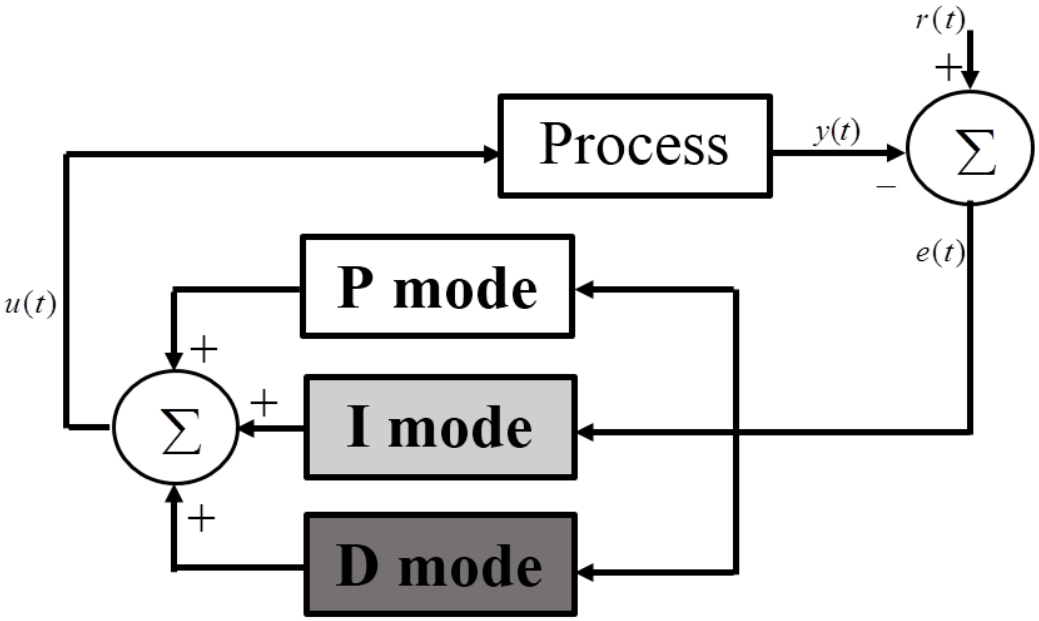

Figure 3.14 Block diagram of a PID controller in feedback control system

P mode or proportional term produces controlled variable which is proportional to the current error value. The proportional response can be adjusted by multiplying the error values by a constant K_c which is called as a proportional gain constant. The proportional term is given by:

$$\text{P mode} = K_c \cdot e(t) \tag{38}$$

The proportional gain K_c is high, it will result in the controlled variable to have large change for a given change in the error values. If the proportional gain K_c is too high, the control system will encounter unstable. On the other hand, the low proportional gain K_c results in a small response of controlled variable to the large error values. Moreover, if the proportional gain K_c is too low, the manipulated variable may be too small when responding to disturbances.

I mode or integral term is directly proportional to both the magnitude of the error values and the period of the error values. The integral in the PID controller is the sum of the instantaneous error values all the time and gives the accumulated offset which has been corrected previously. The accumulated error values are then multiplied by an integral gain K_i. The integral term is given by:

$$\text{I mode} = K_i \cdot \int_o^t e(t) \cdot dt \tag{39}$$

The integral term accelerates the movement of the process towards set-point and eliminates the residual error values which occur with a pure proportional controller. However, the integral term responds to accumulated error values from the past, it can cause the present values to overshoot the set-point values, namely offset elimination.

D mode or derivative term is calculated by determining the slope of the error values all the time and multiplying this rate of change by a derivative gain K_d. The derivative term is given by:

$$\text{D mode} = K_d \cdot \frac{de(t)}{dt} \tag{40}$$

The derivative term predicts behavior of the control system and improves setting time and stability of the control system. However, derivative term is hardly used in practice because it has impact on stability of the control system(Kiam Heong et al., 2005).

3.4.2 SIMC tuning rules

SIMC tuning rules introduced by (Skogestad, 2003) are regarded as one of tuning rules that are proper to calculate PI controller settings, namely proportional gain K_c and integral gain K_i because these tuning rules have degree of freedom that can adjust control action as conservative action or aggressive action. For steps for calculating PI controller settings using SIMC tuning rules, it is necessary to know the models of process, first order plus time delay (FOPDT) or second order plus time delay (SOPDT). The transfer functions of FOPDT and SOPDT are given by:

$$G(s) = \frac{k}{\tau_1 s + 1} e^{-\theta s} \tag{41}$$

$$G(s) = \frac{k}{(\tau_1 s + 1)(\tau_2 s + 1)} e^{-\theta s} \tag{42}$$

These models can be calculated by step test which changes input or manipulated variable suddenly affecting to output or controlled variable. The illustrative step test of FOPDT process is shown in Figure 3.15.

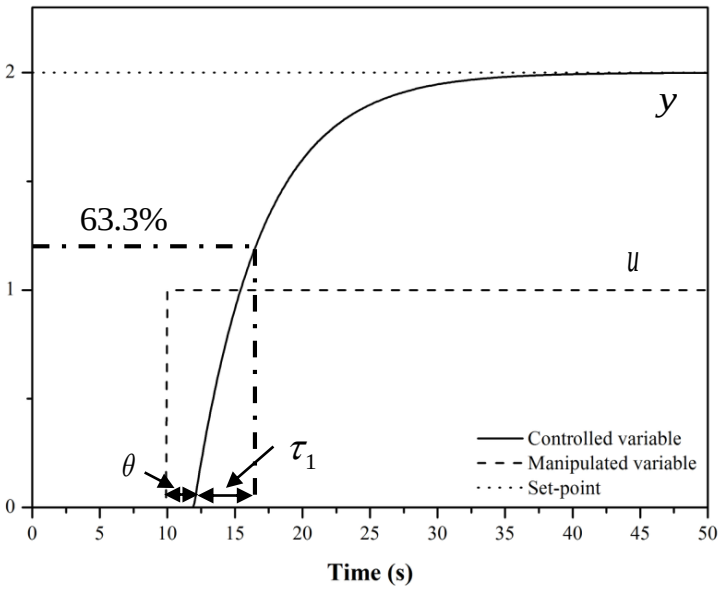

Figure 3.15 The illustrative step test of FOPDT process

Time delay and time constant of FOPDT process can be directly measured after step test, as shown in Figure 3.15. Moreover, process gain of FOPDT process, it can be calculated by:

$$k = \frac{\Delta y}{\Delta u} \tag{43}$$

After a model of FOPDT process has been already calculated, the next step is calculations of proportional gain K_c and integral gain K_i that can be calculated by:

$$K_c = \frac{\tau_1}{k} \cdot \frac{1}{(\theta + \tau_c)} \tag{44}$$

$$K_i = \frac{K_c}{\tau_I}, \ \tau_I = \min(\tau_1, 4(\tau_c + \theta)) \tag{45}$$

The choice of design parameter τ_c is a key decision in SIMC tuning rules. This parameter can adjust desirable controlled variable. Generally, increasing τ_c produces a more conservative controller because proportional gain K_c decreases while τ_I

increases, the responses of closed-loop FOPDT by increasing τ_c can be seen in Figure 3.16. However, there are several IMC guidelines for design parameter τ_c that have been published for the FOPDT process, as given by:

$$\frac{\tau_c}{\theta} > 0.8 \; and \; \tau_c > 0.1\tau \tag{46}$$

$$\tau > \tau_c > \theta \tag{47}$$

$$\tau_c = \theta \tag{48}$$

For more general process models with a dominant time constant, τ_{dom} , equation 47 can be generalized as:

$$\tau_{dom} > \tau_c > \theta \tag{49}$$

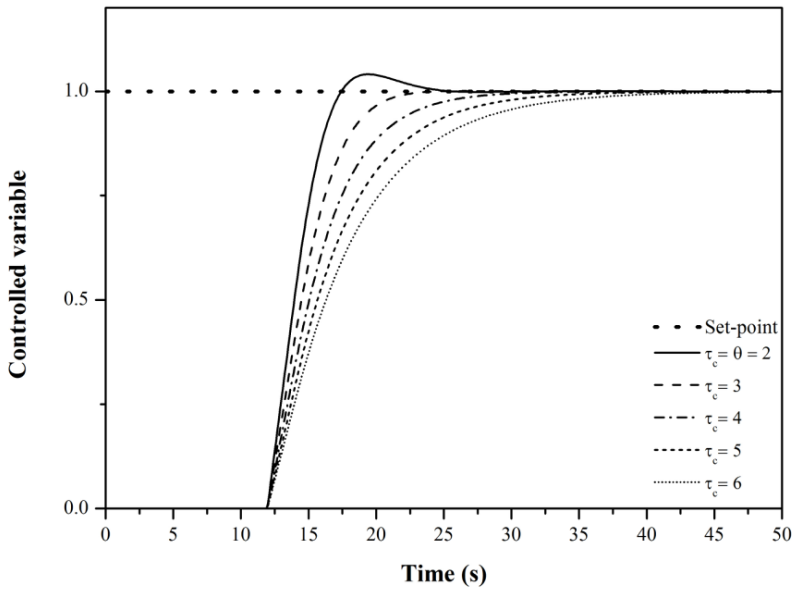

Figure 3.16 The responses of closed-loop FOPDT by increasing τ_c

Chapter IV

Simulation and CPA

In this chapter, the details regarding wind turbine simulation and all steps of CPA will be provided. The simulation used FAST 7 simulator in MATLAB-Simulink represents wind turbine in this work. Moreover, characteristics, control systems and wind speed used in simulation will be discussed in following sections.

4.1 Wind turbine simulation

FAST 7 simulator developed by NREL is used in this simulation and performed in Intel Core i-7 (2.5 GHz), 4 GB RAM within Matlab R2013a. This simulator has three manipulated variables and one controlled variable. Those are torque, pitch, yaw and rotor speed respectively. However, yaw control system is neglected in this work because it is hardly employed to regulate wind turbine in practice. Therefore, torque and pitch control system are only used to regulate wind turbine in this work. The scheme of two control systems to regulate wind turbine is shown in Figure 4.1.

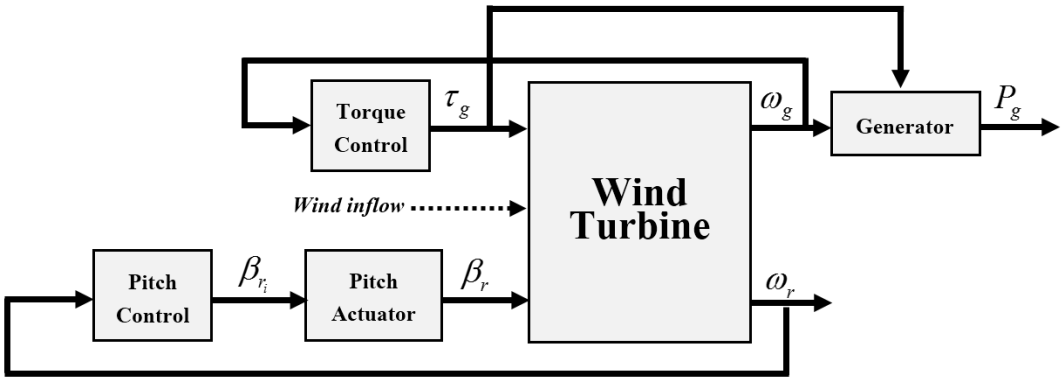

Figure 4.1 The scheme of two control systems in wind turbine

The characteristics of wind turbine in this simulation are corresponded to AWT-27 wind turbine installed in Tehachapi, California, USA, as shown in Table 4.1. The 27.5 meter its diameter rotor rotates at a nominal speed 63.33 rpm. It consists of two blades and a gearbox device.

Rated power	250 kW
Rotor diameter	27.5 m
Number of blades	2
Height of tower	42 m
Cut-in, Rated, Cut-out Wind Speed	4.5 m/s, 12 m/s, 25 m/s
Gearbox ratio	22.5
Nominal rotor speed	63.33 rpm

Table 4.1 Characteristics of wind turbine

The wind inflow used in this simulation consists of 2000 seconds data set of normal wind speed at hub-height. The normal wind speed is assumed in a range of 10 to 15 m/s and comes to confront perpendicularly rotor only. The profile of normal wind speed is shown in Figure 4.2.

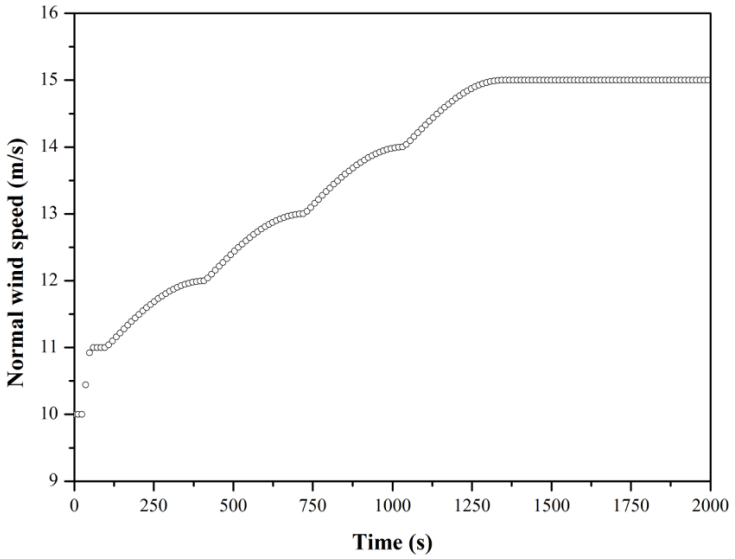

Figure 4.2 The profile of normal wind speed in a range of 10 to 15 m/s

The generator model in this simulation is used as induction generator. The electrical power produced by the induction generator is given by:

$$\mathrm{P}_g = \eta_g \cdot \omega_g \cdot \tau_g \tag{50}$$

where η_g is the generator efficiency, ω_g is the generator speed and τ_g is the generator torque.

There are two blades of wind turbine in this simulation. Therefore, two hydraulic pitch actuators are modeled as a second order transfer function between pitch angle β and its reference β_{r_i} (Shaker and Patton, 2014). The hydraulic pitch actuator is given by:

$$\frac{\beta_r(s)}{\beta_{r_i}(s)} = \frac{\omega_n^2}{s^2 + 2 \cdot \zeta \cdot \omega_n \cdot s + \omega_n^2} \text{ , i = 1,2} \tag{51}$$

where ζ is the damping factor and ω_n is the natural frequency. This transfer function is associated with control system of every blade in pitch systems. For the healthy pitch system, the parameters ζ = 0.6 and ω_n = 11.11 rad/s are used. If a fault of pitch actuator happens, these parameters will change.

จุฬาลงกรณ์มหาวิทยาลัย
Chulalongkorn University

4.2 Control regimes

For torque control system, a induction generator in a wind turbine contains a torque controller. This controller receives generator speed as input and delivers generator torque as output in order to maintain the optimal rotor speed in partial load regime. The generator torque delivered by an induction generator is given by:

$$\tau_g = \frac{\left(\omega_g - \omega_s\right) \cdot \tau_{rated}}{\omega_{rated} - \omega_s} \tag{52}$$

where τ_g is the generator torque, ω_s is the synchronous speed, τ_{rated} is the rated torque and ω_{rated} is the rated generator speed. This generator torque has its limitation at a maximum of 1750 Nm. The synchronous speed, rated torque and rated generator speed for a induction generator used in this simulation are 125.6 RPM, 136.79 Nm and 127.5 RPM, respectively.

For pitch control, it is needed to assist torque control by regulating the output power of the wind turbine and also by keeping the rotor speed within its allowable limit. For this simulation, a simple PI controller is used:

$$\beta_{r_i} = K_p\left(\omega_{nr} - \omega_r\right) + K_I \int_0^t \left(\omega_{nr} - \omega_r\right) dt \tag{53}$$

where ω_{nr} is the nominal rotor speed which the rated power of wind turbine is obtained, ω_r is the measured rotor speed, K_p and K_I are paremeters of PI controller according to SIMC tuning rules (Skogestad, 2003). In order not to exceed the mechanical limitations of the hydraulic pitch actuator, the input signal β_{r_i} is saturated at a maximum of 45º and a rate limit of 8º/sec.

Chulalongkorn University

4.3 Scenarios of faulty pitch actuator and a fluctuation of wind speed

These two scenarios, faulty pitch actuator and fluctuation of wind speed, will be used for investigating CPA in this simulation. Normally, when faulty pitch actuator occurs in the pitch control system, it is manipulated more slowly than healthy pitch actuator. Therefore, the model of faulty pitch actuator is modelled as second order transfer function plus time delay, as given by:

$$\frac{\beta_r(s)}{\beta_{r_i}(s)} = \frac{\omega_n^2}{s^2 + 2\cdot\zeta\cdot\omega_n\cdot s + \omega_n^2} e^{-\theta S} \quad , \text{i} = 1,2 \tag{54}$$

where ζ is the damping factor, ω_n is the natural frequency and θ is the time delay. Moreover, If a fault of pitch actuator happens, the damping factor and natural frequency will be change as ζ = 5, ω_n = 5.47 rad/s and θ=6.5 s.

For scenario of the fluctuation of wind speed, the normal wind speed shown in Figure 4.2 is introduced by white noise with variance is equal to 1. The profile of the fluctuation of wind speed is shown in Figure 4.3.

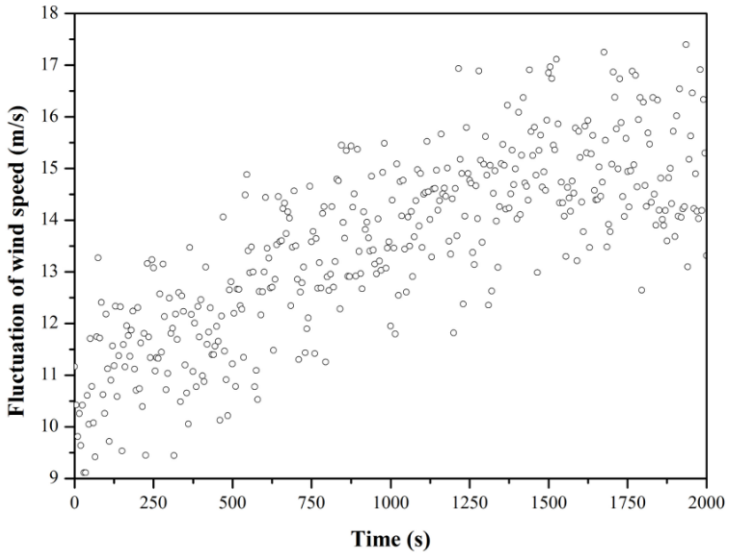

Figure 4.3 The profile of the fluctuation of wind speed

4.4 CPA for pitch control system

For using CPA to detect both the fluctuation of wind speed and the faulty pitch actuator affecting to the performance of the pitch control system. Closed loop data of PI pitch control system, manipulated variable and controlled variable, will be collected for calculating the performance index, as shown in Figure 4.4. The benchmark used to measure the performance of pitch control system is minimum variance index. The linear black-box model, AR model, is used to represent the real system with order $n = 30$. The sampling time and data length used for collecting the data of closed loop system are 0.1 s and 1500 samples. For calculation of the performance index, every data length of 1500 samples collected will be computed the performance index.

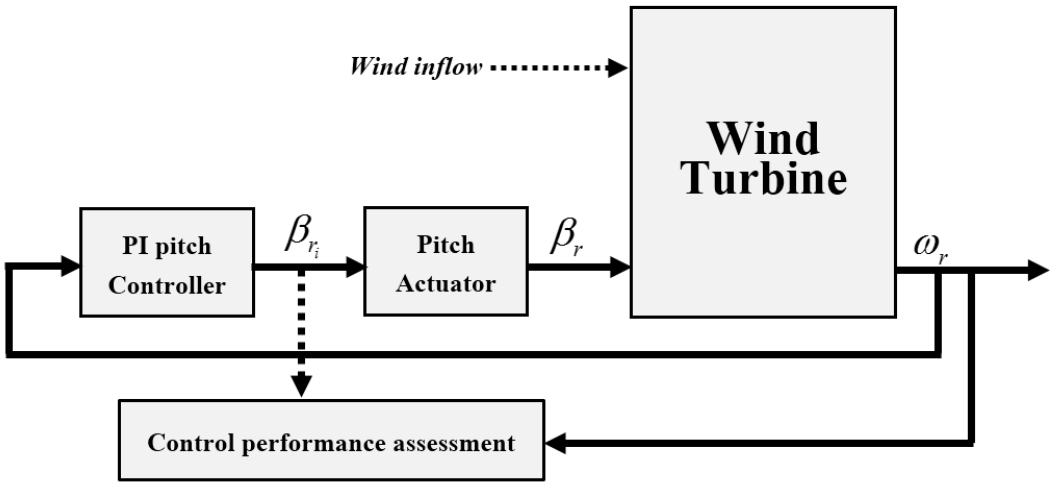

Figure 4.4 The scheme of collected closed loop data

4.5 Robustness assessment for pitch control system

In this section, an algorithm of robustness assessment used to measure the robustness of PI pitch control system will be discussed. The robustness assessment for PI pitch control system will be measured as on-line measurement. Therefore, in order to understand regarding an algorithm of the on-line robustness assessment, the algorithm of robustness assessment for FOPDT will be presented. FOPDT closed loop system shown in Figure 4.5 will be considered. The process G_P is regulated by the PI controller G_c with constant set-point. Moreover, the disturbance w is add at controlled variable.

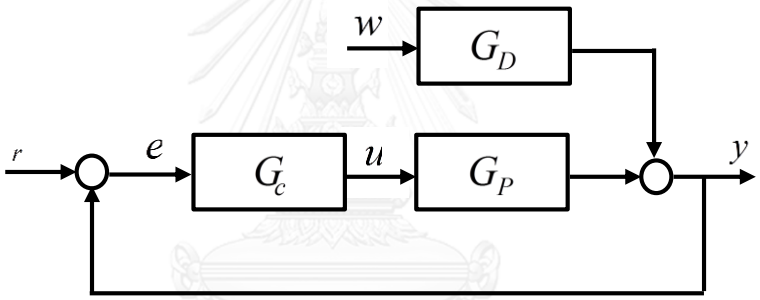

Figure 4.5 Block diagram of the FOPDT closed loop system

The transfer function of FOPDT is given by:

$$G_P(s) = \frac{k}{\tau_1 s + 1} e^{-\theta s} \tag{55}$$

Where k is the process gain, τ_1 is the time constant of process and θ is the time delay of process.

The transfer function of PI controller is given by:

$$G_c(s) = K_c + \frac{K_c}{\tau_I s} \tag{56}$$

Where K_c the proportional is gain and τ_I is the integral time.

The disturbance is s white noise w with variance σ_w^2 , which is filtered through a first-order lag with time constant τ_N :

$$G_D(s) = \frac{1}{\tau_N s + 1} \tag{57}$$

For the FOPDT closed loop system, the error $e(s)$ and its power spectrum density $S_e(j\omega)$ can be calculated by:

$$S(s) = \frac{1}{(1 + G_P(s)G_c(s))} \tag{58}$$

$$e(s) = S(s) \cdot G_D(s) \cdot w(s) \tag{59}$$

$$S_e(j\omega) = \left|S(j\omega)G_D(j\omega)\right|^2 \sigma_w^2 \tag{60}$$

where $S(s)$ is the sensitivity function

the PI controller G_c tuned corresponds to SIMC tuning rules. The integral time is set equal to the time constant of process, as given:

$$\tau_I = \tau_1 \tag{61}$$

จุฬาลงกรณ์มหาวิทยาลัย
Chulalongkorn University

In example of FOPDT process, $k = 1, \tau_1 = 1, \theta = 0.5, \sigma_w^2 = 1$ and $\tau_N = 10$, when the proportional gain K_c is increased, the power spectrum density of the error e changes accordingly, as shown in Figure 4.6. As the proportional gain K_c is increased, the oscillation in the frequency range around the phase crossover frequency ω_c appear obviously because the gain margin is decreased. The phase crossover frequency ω_c for the constant integral time $\tau_I = \tau_1$ can be obtained by:

$$\omega_c = \frac{\pi}{2\theta} \tag{62}$$

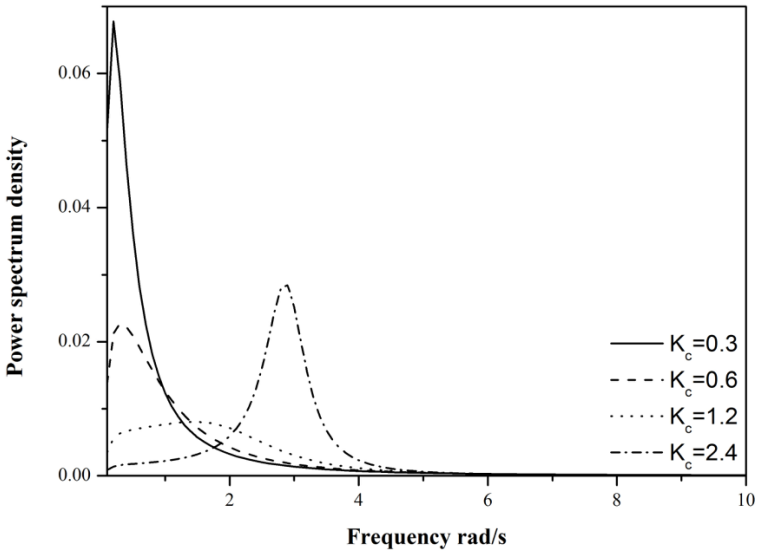

Figure 4.6 Power spectrum density of the error for the PI controller

The information of the signal power in this frequency range is used to measure the robustness of FOPDT closed loop system. The signal power ratio ρ of the power in the frequency range around ω_c is defined as:

$$\rho = \frac{\int_{\omega_{\min}}^{\omega_{\max}} S_e(\omega) d\omega}{\int_0^{\infty} S_e(\omega) d\omega}, \ \omega_{\min} < \omega_c < \omega_{\max} \tag{63}$$

Note that the quantity is normalized by the total power in order to eliminate the effect of the noise variance σ_ω^2 . The frequency range is chosen as $0.5\omega_c$ and $2\omega_c$.

The relations between the proportional gain K_c and the signal power ratio ρ are shown in left hand plot of Figure 4.7. The relations between the signal power ratio ρ and maximum sensitivity M_{ST} are shown in right hand plot of Figure 4.7. The maximum sensitivity M_{ST} is well known to be good measurement to indicate the trade-

off between the performance and robustness. In addition, the maximum sensitivity M_{ST} that indicates good robustness is a range of 1.2 to 2(Åström and Hägglund, 2006).

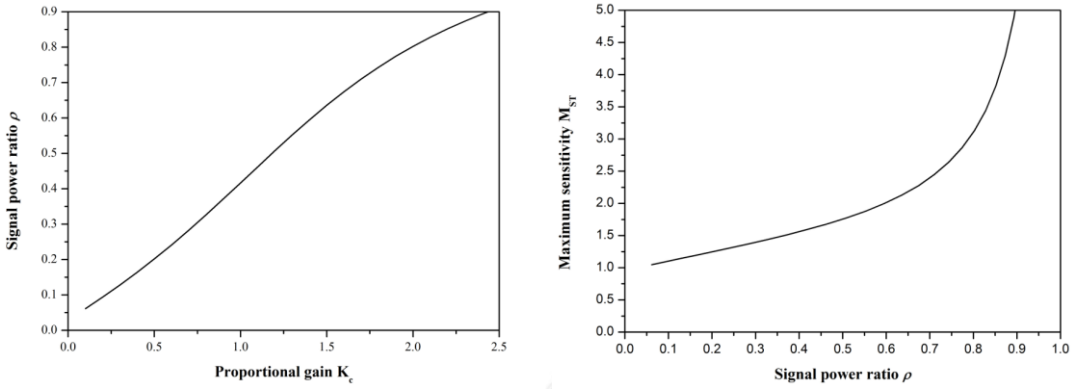

Figure 4.7 The relations between proportional gain/signal power ratio and signal power ratio/maximum sensitivity

From Figure 4.7, it can imply that the robustness of FOPDT closed loop system can be measured by calculation of signal power ratio ρ that is a function of the maximum sensitivity M_{ST}. The signal power ratio can be directly calculated from the error signal by using digital signal technique, as given by:

$$\rho(k) = \frac{\sum_{i=k-N}^{k} e_f^2(i)}{\sum_{i=k-N}^{k} e^2(i)} \tag{64}$$

where N is s window length, e_f is the filtered signal and e is the error signal. The filtered signal e_f can be obtained by using a band pass filter, whose pass band is a range of $\omega_{\min}$ to $\omega_{\max}$.

For on-line robustness assessment of PI pitch control system, the phase crossover frequency calculated is 0.5 rad/s, pass band filter is employed with band pass in a range of 0.25 to 1 rad/s and window length for calculation of power signal ratio is set equal to 200.

Chapter V

Results and discussion

In this chapter, the results and discussion regarding effects of a faulty pitch actuator and a wind speed fluctuation on the performance detected by CPA of the pitch control system will be presented. In addition, effects of faulty pitch actuator and a wind speed fluctuation on the robustness of the PI pitch control system will be also presented.

From the simulation, pitch control system in wind turbine is regulated by PI controller. Therefore, PI controller settings, proportional gain K_c and integral time τ_I are required to calculate before performing the simulation. Calculation of PI controller settings used step test method to estimate a model of wind turbine system. In step test method, the pitch angel was swiftly changed from 0 degree to 5.729 degree resulting in the rotor speed decreased from 114.7 rpm to 86 rpm. From obtained response of the rotor speed shown in Figure 5.1, it can be used to estimate a model of wind turbine system.

จุฬาลงกรณ์มหาวิทยาลัย
Chulalongkorn University

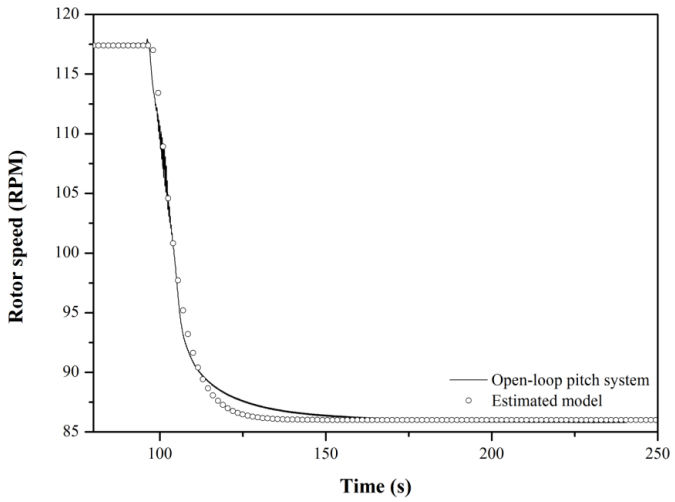

Figure 5.1 The response of rotor speed using step test method

The model of wind turbine system is obtained as:

$$G_p(s) = \frac{-314e^{-3s}}{8.8s+1} \tag{67}$$

The model of wind turbine system is then used to calculate PI controller settings corresponding to SIMC tuning rules in order to use for pitch control system in studies of two scenarios, the faulty pitch actuator and fluctuation of wind speed. PI controller settings obtained are given in Table 5.1.

PI controller settings	
Proportional gain K_c	-0.0035
Integral time τ_I	8.8

Table 5.1 PI controller settings

5.1 Effects of a fluctuation of wind speed on the performance of the pitch control system

In investigation of CPA based on minimum variance index to detect fluctuation of wind speed affecting to the performance of the PI pitch control system. The healthy pitch actuator is employed in PI pitch control system for this scenario. After simulation, the closed-loop data shown in Figure 5.2 of PI pitch control system in the case of normal wind speed and fluctuation of wind speed were collected at 0.1 s sampling rate in a range of 1100 s to 2000 s so that they are used for CPA. The estimated time delay of PI pitch control system was 3 s. The collected data are showed in Figure 5.3.

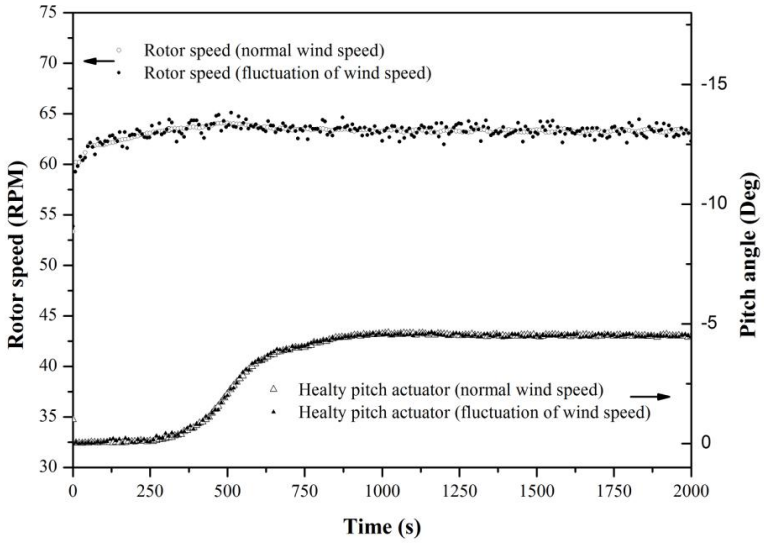

Figure 5.2 The closed-loop data of PI pitch control system in the case of normal wind speed and fluctuation of wind speed.

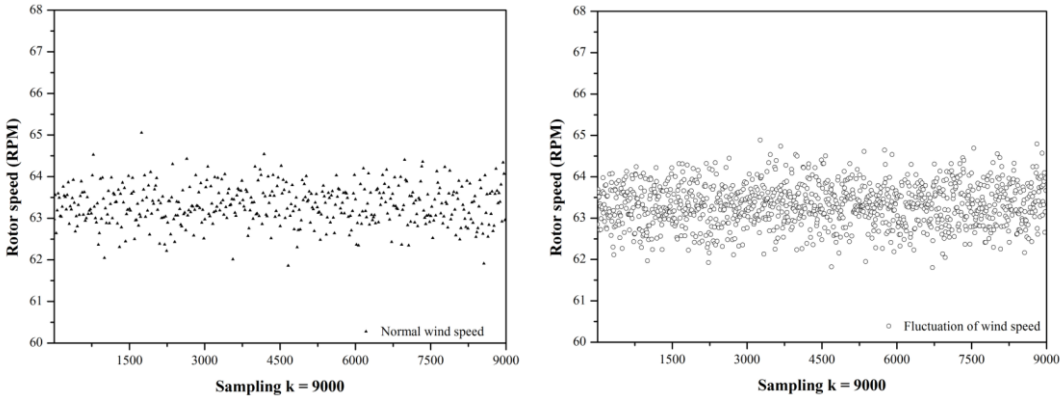

Figure 5.3 Collected data of pitch control system in the case of normal wind speed and fluctuation of wind speed.

Figure 5.4 indicates the performance index detected by CPA between normal wind speed and fluctuation of wind speed. When the control systems of pitch control operate at normal wind speed, the performance of the control system is good around 0.9. However, at fluctuation of wind speed, the performance of the control system decreases significantly because the pitch control cannot manipulate promptly causing the rotor speed to have variation (see Figure 5.2). In order to enhance the performance of the PI

pitch control system, the pitch controller should be tuned as aggressive controller but it can affect the robustness of control system.

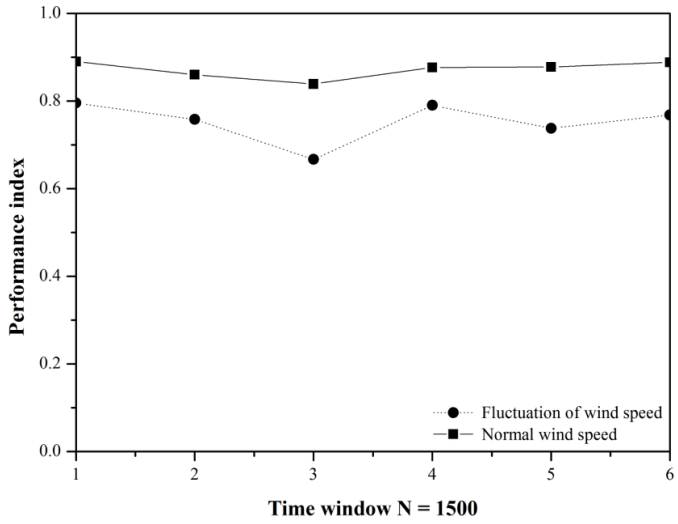

Figure 5.4 Comparisons of the performance index between normal wind speed and fluctuation of wind speed.

5.2 Effects of a faulty pitch actuator on the performance of the pitch control system

For using CPA based on minimum variance index to detect faulty pitch actuators affecting to the performance of the pitch control system, the closed-loop data shown in Figure 5.5 of PI pitch control system in the case of faulty and healthy pitch actuators used for CPA were collected at 0.1 s sampling rate in a range of 1100 s to 2000 s. The estimated time delay of PI pitch control system was 3 s. The collected data are showed in Figure 5.6.

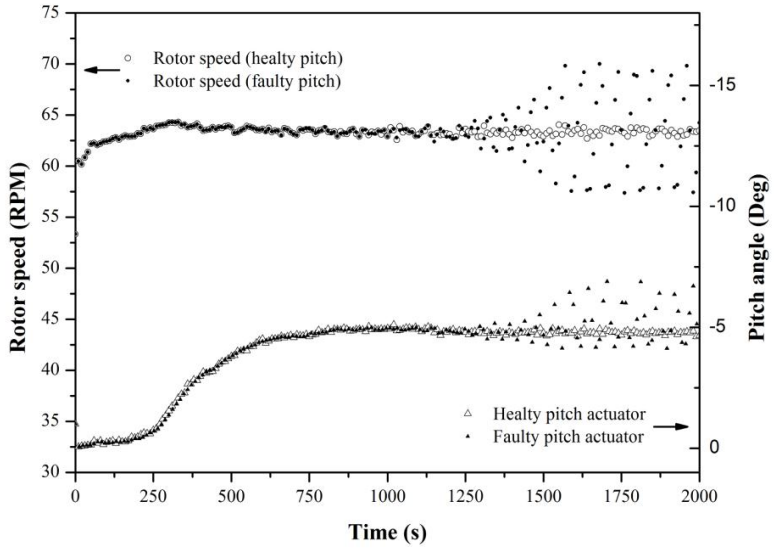

Figure 5.5 The closed-loop data of pitch control system in the case of faulty and healthy pitch actuators

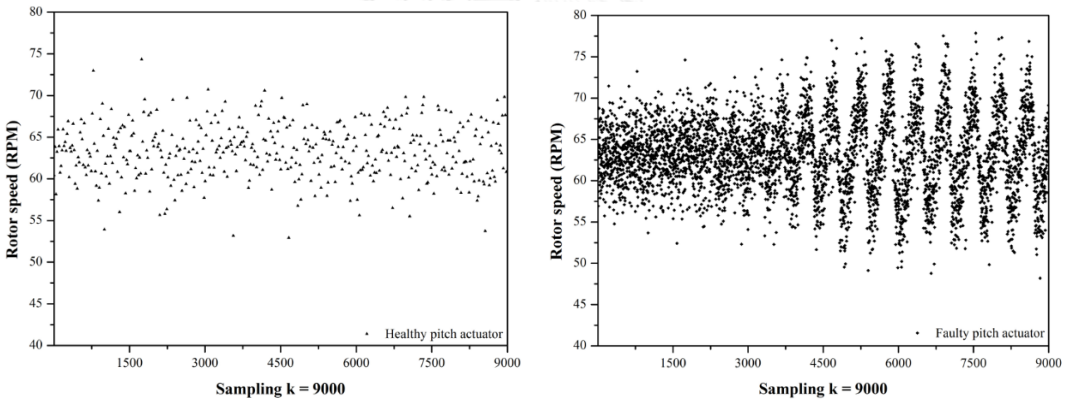

Figure 5.6 Collected data of pitch control system in the case of faulty and healthy pitch actuators

Figure 5.7 indicates the performance index detected by CPA between healthy pitch actuator and a faulty pitch actuator. Both scenarios were performed at normal wind speed. When pitch actuators is healthy, pitch control system can regulate effectively the rotor speed throughout the range of wind speed. The performance of pitch control system is good around 0.9. However, when pitch actuators is faulty, pitch control system cannot regulate effectively the rotor speed at wind speed reaches 15 m/s at time

1250 s. As a result, the performance of pitch control system decreases significantly. Moreover, it results in the rotor speed to have high oscillation at time in range of 1250 s to 2000s. (See Figure 5.5). Therefore, it can be concluded that CPA can detect effectively the performance of pitch control system in case of healthy pitch actuator and a faulty pitch actuator.

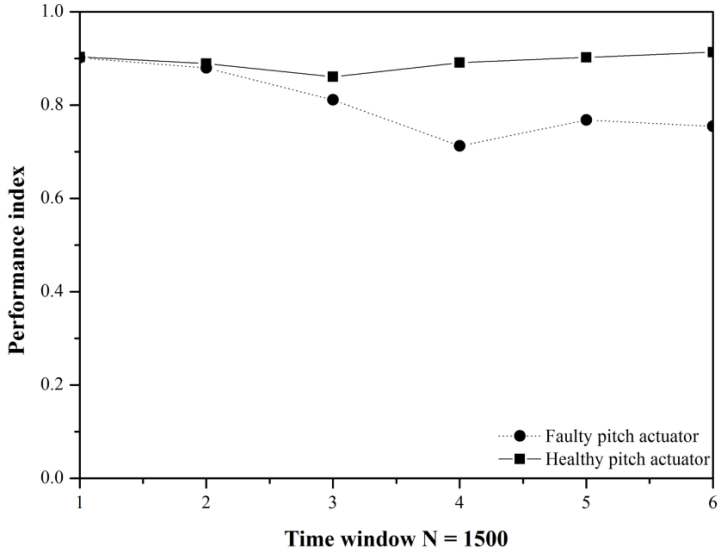

Figure 5.7 Comparisons of the performance index between healthy and a faulty pitch actuator.

จุฬาลงกรณ์มหาวิทยาลัย
Chulalongkorn University

5.3 Effects of a fluctuation of wind speed and faulty pitch actuator on the robustness of the pitch control system

For investigation of the robustness of PI pitch control system, the robustness will be measured as on-line measurement. In on-line robustness assessment of PI pitch control system, it is required to find the relations shown in Figure 5.8 and Figure 5.9 of proportional gain K_c / the signal power ratio ρ and signal power ratio ρ / maximum sensitivity M_{ST} in order that the signal power ratio ρ relating to maximum sensitivity M_{ST} will be used to indicate the robustness of the PI pitch control system.

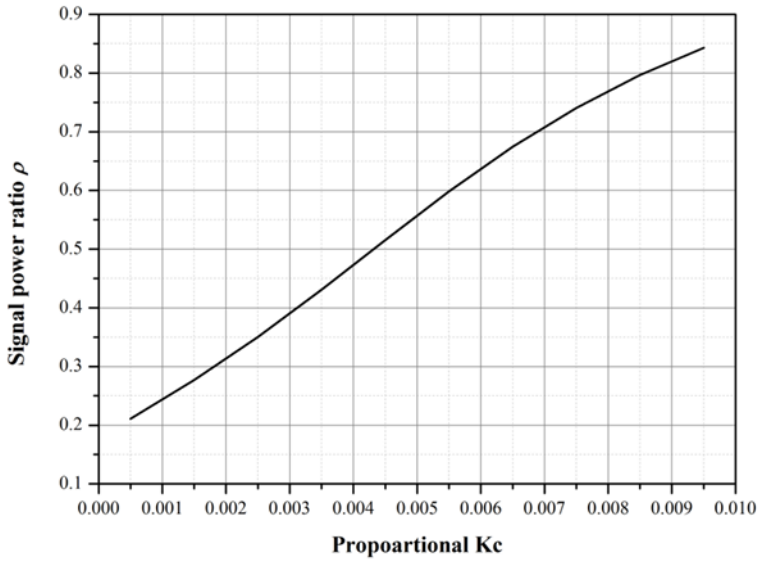

Figure 5.8 The relations between proportional gain and signal power ratio and signal power.

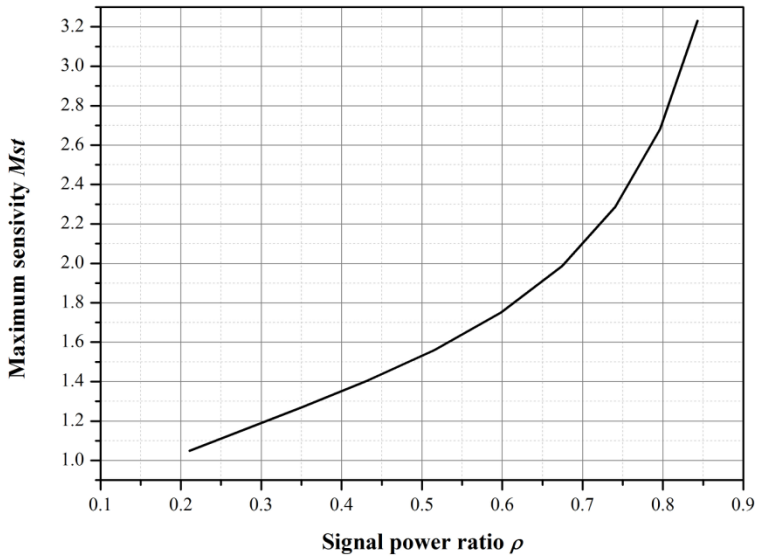

Figure 5.9 The relations between signal power ratio and maximum sensitivity of PI pitch control system.

The on-line robustness assessment is used to measure the robustness of PI pitch control system in cases of normal wind speed, fluctuation of wind speed, healthy pitch actuator and faulty pitch actuator in period from 1300 s to 2000 s, as shown in Figure 5.2 and 5.5. For scenarios of normal wind speed and fluctuation of wind speed, the healthy pitch actuator is employed in PI pitch control system. Controller settings, proportional gain K_c and integral time τ_I used correspond to Table 5.1. From on-line robustness assessment in case of a normal wind speed, the results showed that the signal power ratio corresponding to proportional gain K_c=0.0035 of PI pitch controller used in simulation is approximately 0.42, as shown in Figure 5.10. In addition, signal power ratio of 0.42 can be converted to maximum sensitivity of 1.4 by using the relations between signal power ratio and maximum sensitivity for PI pitch control system, as shown in Figure 5.9. However, when PI pitch control system undergoes a fluctuation of wind speed, the signal power ratio ρ changes from 0.42 to 0.45. From increase of

signal power ratio, it can implies that PI pitch control system has poor robustness when it faces with disturbances coming in the process. Therefore, in order to keep the robustness of PI pitch control system tuned by SIMC tuning rules, the controller must be tuned with high design parameter τ_c , For example, design parameter τ_c is two times the time delay of process.

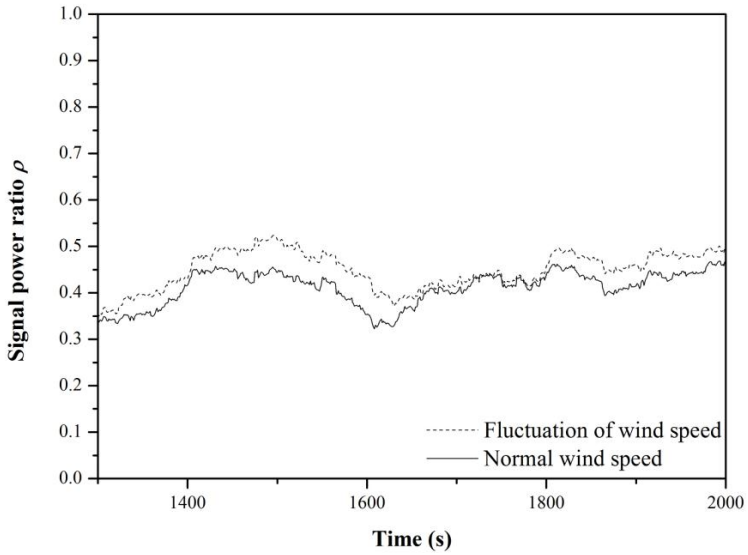

Figure 5.10 Signal power ratio in cases of fluctuation of wind speed and normal wind speed

จุฬาลงกรณ์มหาวิทยาลัย
Chulalongkorn University

For on-line robustness assessment of PI pitch control system in cases of healthy pitch actuator and faulty pitch actuator, the PI pitch control system is performed at normal wind speed. The result showed that when PI pitch control system performs with healthy pitch actuator, power signal ratio is approximately 0.42, as shown in Figure 5.11. In addition, Power signal ratio of 0.42 is equal to maximum sensitivity of 1.4, as shown in Figure 5.9. The maximum sensitivity of 1.4 indicates that the PI pitch control system performed with healthy pitch actuator has fair robustness and is quite conservative. However, when PI pitch control system has to face with faulty pitch

actuator, power signal ratio decreases significantly from 0.42 to 0.12, as shown in Figure 5.11. From decrease of power signal ratio in period from 1600 s to 2000 s, it indicates that PI pitch control system has good robustness but the performance is poor due to faulty pitch actuator resulting in PI pitch control system to have high oscillation, as shown in Figure 5.5. Form investigation of on-line robustness assessment by using two relations based on frequency response analysis in PI pitch control system of wind turbine system, it can be concluded that this algorithm can indicate the robustness of PI pitch control system effectively.

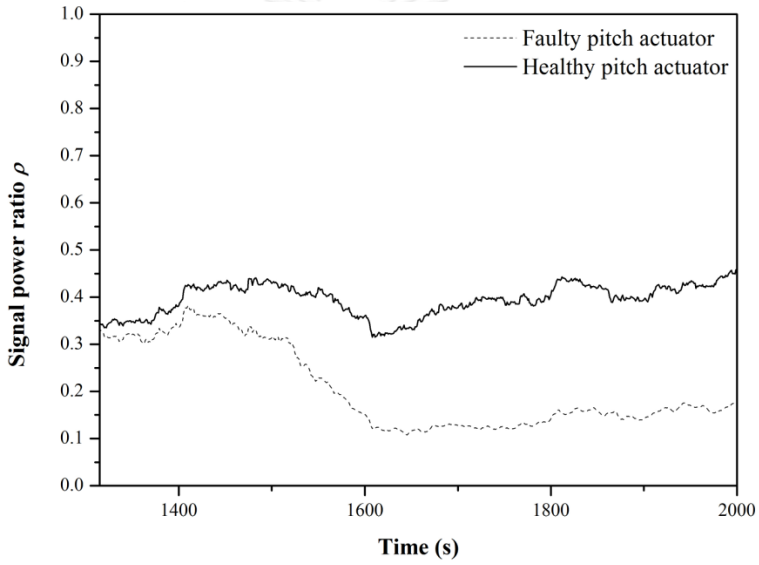

Figure 5.11 Signal power ratio in cases of faulty and healthy pitch actuators

Chapter VI

Conclusion and recommendation

6.1 Conclusion

In this work, the main objective is to investigate the use of CPA techniques in wind turbine system. By investigation of CPA techniques, it is used to detect the performance of two effects, a faulty pitch actuator and a wind speed fluctuation acting on the PI pitch control system in wind turbine. In addition, the on-line robustness assessment is used to measure the robustness of PI pitch control system.

The CPA techniques used minimum variance index are a benchmark in measurement of the performance of PI pitch control system. The data length and sampling time to collect closed loop data are 1500 samples and 0.1 s per sample. For the on-line robustness assessment, frequency response techniques are adapted to measure the robustness in type of two relations, the signal power ratio ρ and maximum sensitivity M_{ST}.

จุฬาลงกรณ์มหาวิทยาลัย
Chulalongkorn University

The results showed that the use of CPA techniques can indicates effectively the performance of the pitch control system in case of a faulty pitch actuator and a wind speed fluctuation acting on the pitch control system in wind turbine. For the on-line robustness assessment, it can indicate effectively the robustness of PI pitch control system when a faulty pitch actuator and a wind speed fluctuation acts on the system as well.

6.2 Recommendation

For investigation of the on-line robustness assessment, various parameters involving in calculation of power signal ratio have to study regarding suitable parameters in order to be able to measure accurately the robustness of the PI pitch control system, such as filter order and window length. Moreover, the algorithm of on-line robustness assessment has to compare with other algorithms involved with robustness assessment in order to point the differences between this algorithm and other algorithms.

จุฬาลงกรณ์มหาวิทยาลัย
Chulalongkorn University

REFERENCES

Ackermann, T. and L. Söder (2000). "Wind energy technology and current status: a review." Renewable and Sustainable Energy Reviews **4**(4): 315-374.

Åström, K. J. and T. Hägglund (2006). Advanced PID Control, ISA-The Instrumentation, Systems, and Automation Society.

Attya, A. B. and T. Hartkopf (2012). "Penetration impact of wind farms equipped with frequency variations ride through algorithm on power system frequency response." International Journal of Electrical Power & Energy Systems **40**(1): 94-103.

Boukhezzar, B., L. Lupu, H. Siguerdidjane and M. Hand (2007). "Multivariable control strategy for variable speed, variable pitch wind turbines." Renewable Energy **32**(8): 1273-1287.

Boukhezzar, B. and H. Siguerdidjane (2010). "Comparison between linear and nonlinear control strategies for variable speed wind turbines." Control Engineering Practice **18**(12): 1357-1368.

Carelli, A. C. and M. B. de Souza Jr (2009). Stochastic and Deterministic Performance Assessment of PID and MPC Controllers: Application to a Hydrotreater Reactor. Computer Aided Chemical Engineering. C. A. O. d. N. Rita Maria de Brito Alves and B. Evaristo Chalbaud, Elsevier. **Volume 27:** 1635-1640.

Chen, B., P. C. Matthews and P. J. Tavner (2013). "Wind turbine pitch faults prognosis using a-priori knowledge-based ANFIS." Expert Systems with Applications **40**(17): 6863-6876.

Desborough, L. and T. Harris (1992). "Performance assessment measures for univariate feedback control." The Canadian Journal of Chemical Engineering **70**(6): 1186-1197.

Garpinger, O., T. Hägglund and K. J. Åström (2014). "Performance and robustness trade-offs in PID control." Journal of Process Control **24**(5): 568-577.

Goradia, D. B., S. Lakshminarayanan and G. P. Rangaiah (2005). "Attainment of PI Achievable Performance for Linear SISO Processes with Deadtime by Iterative Tuning." The Canadian Journal of Chemical Engineering **83**(4): 723-736.

Grimble, M. J. (2002). "Controller performance benchmarking and tuning using generalised minimum variance control." Automatica **38**(12): 2111-2119.

Hameed, Z., Y. S. Hong, Y. M. Cho, S. H. Ahn and C. K. Song (2009). "Condition monitoring and fault detection of wind turbines and related algorithms: A review." Renewable and Sustainable Energy Reviews **13**(1): 1-39.

Harris, T. J. (1989). " Assessment of Control Loop Performance." The Canadian Journal of Chemical Engineering **67**: 856-861.

Hoo, K. A., M. J. Piovoso, P. D. Schnelle and D. A. Rowan (2003). "Process and controller performance monitoring: overview with industrial applications." International Journal of Adaptive Control and Signal Processing **17**(7-9): 635-662.

Horch (2000). "Condition Monitoring of Control Loops." PhD Thesis Royal Institute of Technology, Stockholm, Sweden.

Huang, B. and S. L. Shah (1999). "Performance assessment of control loops." Berlin: Springer.

Jelali, M. (2006). "An overview of control performance assessment technology and industrial applications." Control Engineering Practice **14**(5): 441-466.

Jelali, M. (2007). "Performance assessment of control systems in rolling mills – application to strip thickness and flatness control." Journal of Process Control **17**(10): 805-816.

Jin, Q., Q. Liu, Q. Wang, Y. Tian and Y. Wang (2013). "PID Controller Design Based on the Time Domain Information of Robust IMC Controller Using Maximum Sensitivity." Chinese Journal of Chemical Engineering **21**(5): 529-536.

Kiam Heong, A., G. Chong and L. Yun (2005). "PID control system analysis, design, and technology." IEEE Transactions on Control Systems Technology **13**(4): 559-576.

Kusiak, A. and A. Verma (2011). "A Data-Driven Approach for Monitoring Blade Pitch Faults in Wind Turbines." Sustainable Energy, IEEE Transactions on **2**(1): 87-96.

Nejad, A. R., Z. Gao and T. Moan (2014). "Fatigue Reliability-based Inspection and Maintenance Planning of Gearbox Components in Wind Turbine Drivetrains." Energy Procedia **53**: 248-257.

Patwardhan, R. S., S. Shah, G. Emoto and H. Fujii (1998). "Performance analysis of model-based predictive controllers: An industrial study." Proceedings of the AIChE.

Shaker, M. S. and R. J. Patton (2014). A Fault Tolerant Control Approach to Sustainable Offshore Wind Turbines. Wind Turbine Control and Monitoring. N. Luo, Y. Vidal and L. Acho. Cham, Springer International Publishing**:** 157-190.

Singh, M., E. Muljadi, J. Jonkman and V. Gevorgian (2014). "Simulation for Wind Turbine Generators—With FAST and MATLAB-Simulink Modules." National Renewable Energy Laboratory (NREL).

Skogestad, S. (2003). "Simple analytic rules for model reduction and PID controller tuning." Journal of Process Control **13(**4): 291-309.

Thornhill NF, O., Fedenczuk MS (1999). "Refinery-wide control loop performance assessment." Journal of Process Control **9**: 109-124.

Viveiros, C., R. Melício, J. M. Igreja and V. M. F. Mendes (2014). "Performance Assessment of a Wind Turbine Using Benchmark Model: Fuzzy Controllers and Discrete Adaptive LQG." Procedia Technology **17**(0): 487-494.

Zhang, Z. and L.-S. Hu (2012). "Performance assessment for the water level control system in steam generator of the nuclear power plant." Annals of Nuclear Energy **45**: 94-105.

จุฬาลงกรณ์มหาวิทยาลัย
Chulalongkorn University

APPENDIX

จุฬาลงกรณ์มหาวิทยาลัย
Chulalongkorn University

Appendix A: MATLAB Codes-Simulink

Appendix A.1: Control systems of wind turbine system in FAST 7 simulator

- Overall control systems

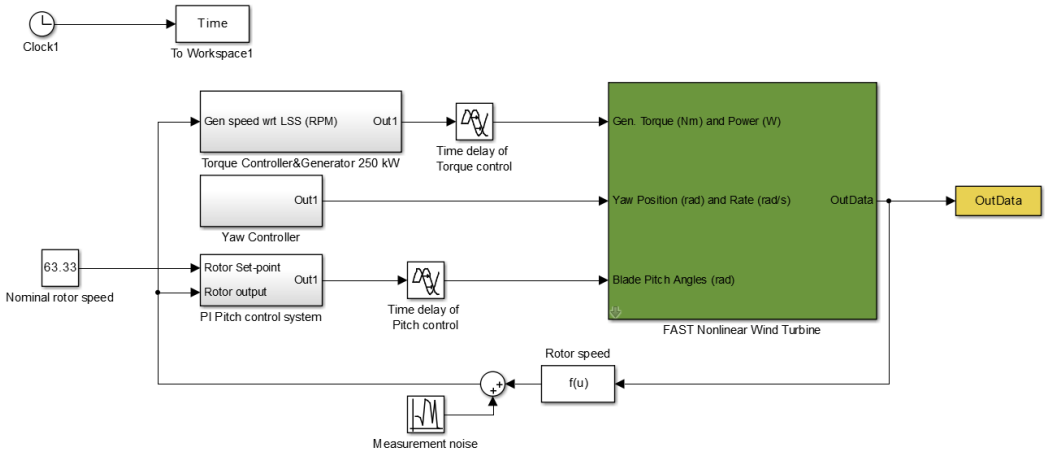

- Torque control and generator 250 kW

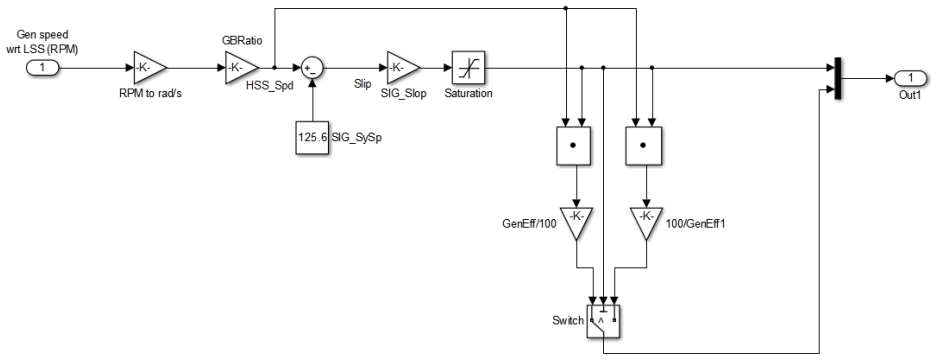

- PI pitch control system

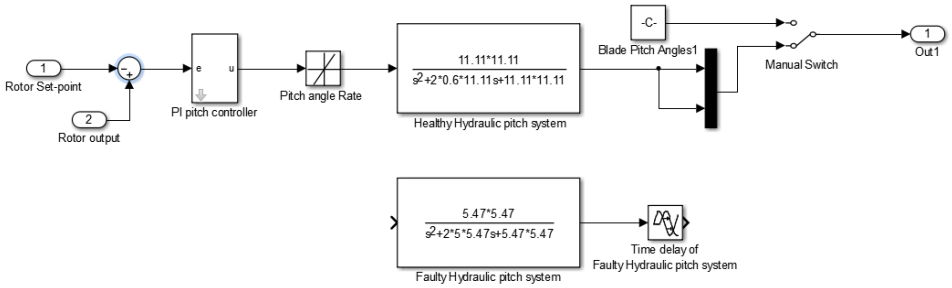

Appendix A.2: CPA code

```
y = PV(11001:20000) % Control variable of process
wind = 1500;
u = [];% Manipulated variable of process
Ts = 0.1;% Sampling time
x = 30; % Order of AR Model
d = 3;% Time dalay
for a = 1:1:(length(y)/wind)+1
    if (a<=(length(y)/wind))
        Y(:,a) = y(1+(a-1)*wind:a*wind);
        yc = Y(:,a);
    else
        Yf = y(1+(a-1)*wind:length(y));
        yc = Yf;
    end
    model = iddata(yc,u,Ts)
    mb = ar(model,x)
    A  = (mb.a)
    e = zeros(1,x+1);
    er = zeros(1,2*length(yc));
    for i = 1:x+1
    if i == 1
        e(1) = A(1);
    else
        for j = 1:i-1
            e(i) = -e(i-j)*A(j+1)+e(i);
        end
    end
end
eem(a) = sum(e(1:d).^2)
eer(a) = sum(e(1:x+1).^2)
for i = 1:length(yc)
    for j = 1:length(A)
        er(j+i-1) = (A(j)*y(i))+er(j+i-1);
    end
end
er = er(1:length(yc));
Disvariance(a) = var(er)
Minimun(a) = eem(a)*Disvariance(a)
Real(a) = eer(a)*Disvariance(a)
PerformanceIndex(a) = Minimun(a)/Real(a)
end
timewindows = 1:1:length(PerformanceIndex);
plot(timewindows,PerformanceIndex(1,:),'--
*k','LineWidth',1,'MarkerEdgeColor','k')
hold on
```

จุฬาลงกรณ์มหาวิทยาลัย
Chulalongkorn University

Appendix A.3: Robustness assessment code

```
clc
clear all
kc = [0.0005:0.001:0.0100];
Ti = 8.8;
w = 0.0001:0.0001:5;
dw = 0.0001;
for k = 1:length(kc)
for i = 1:length(w)
Gol(k,i) = kc(k).*314.*exp(-
3*w(i)*j).*(Ti*w(i)*j+1)./((8.8*w(i)*j+1).*(Ti*w(i)*j));
Ds(k,i) = 1./(10*w(i)*j+1);
end
end
Gcl= (1./(1+Gol)).*Ds;
Mst1 = abs(Gcl);
Mst = (Mst1.^2)*2.11;
tt = w(1:length(w));
Compare = [tt',Mst'];
for i = 1:length(kc)
p(i) =
sum(Compare((2500:10000),i+1)*dw)/sum(Compare(:,i+1)*dw);
end
PP = [p];
figure
plot(kc,PP)
grid on
xlabel('Proportional gain kc')
ylabel('Signal power ratio p')
hold on
%%%%%%%%%%%%%%%%%%%%MST to Ro %%%%%%%%%%
for k = 1:length(kc)
for i = 1:length(w)
Gol2(k,i) =  kc(k).*314.*exp(-
3*w(i)*j).*(Ti*w(i)*j+1)./((8.8*w(i)*j+1).*(Ti*w(i)*j));
end
end
Gcl2 = Gol2./(1+Gol2);
Mst3 = abs(Gcl2);
Mst4 = Mst3';
tt = w(1:length(w));
M = max(Mst4);
Gcl3 = 1./(1+Gol2);
Mst5 = abs(Gcl3);
Mst5 = Mst5';
P = max(Mst5);
MST = max(M,P);
Compare1 = [kc',MST'];
figure
plot(PP,MST)
```

```
grid on
xlabel('Signal power ratio p')
ylabel('Maximum sensivity MST')
ax = gca;
ax.XTick = [0.2 0.4 0.6 0.8];
%%%%%%Chebychev TYPE II bandpass filter%%%%
e1 = e(1101:length(e))';
N = 200;
[b,a] = cheby2(5,5,[0.0796 0.318],'bandpass');
dataIn = e1(1:length(e1),1);
dataOut = filter(b,a,dataIn);
tt = 1:length(dataIn);
for k = 1:length(dataIn)
    if k <= N
    p(k) = sum(dataOut(1:k).^2)/sum(dataIn(1:k).^2);
    elseif k > N
    p(k) = sum(dataOut(k-N:k).^2)/sum(dataIn(k-N:k).^2);
    end
end
subplot(2,1,1)
plot(tt,p,'y')
legend('Ro')
xlabel('Sample')
ylabel('Rho')
hold on
subplot(2,1,2)
plot(tt,dataIn,'g--',tt,dataOut,'y')
legend('Pre-filter','Post-filter')
xlabel('Sample')
ylabel('Error signal')
hold on
```

จุฬาลงกรณ์มหาวิทยาลัย
Chulalongkorn University

VITA

Mr. Chaturawit Chinnachit was born on November 3, 1991 in Prachin Buri province, Thailand. In 2010, he finished secondary school from Chumsaeng Chanutid School, Nakhonsawan, Thailand. After that, he graduated the Bachelor's Degree in Chemical engineering from Rajamangala University of Technology Thanyaburi in 2014. He continued studying the Master's Degree of engineering in Chemical Engineering at Chulalongkorn University and joined Computational Process Engineering Research Center.

จุฬาลงกรณ์มหาวิทยาลัย
Chulalongkorn University